NASA Contractor Report 4230

Detailed Design of a Ride Quality Augmentation System for Commuter Aircraft

Reiner Suikat, Kent E. Donaldson,
and David R. Downing
The University of Kansas Center for Research, Inc.
Flight Research Laboratory
Lawrence, Kansas

Prepared for
Langley Research Center
under Grant NAG1-345

National Aeronautics and
Space Administration
Office of Management
Scientific and Technical
Information Division

1989

Abstract

This report documents the continued design of a Ride Quality Augmentation System (RQAS) for commuter aircraft. The RQAS is designed for a Cessna 402B airplane, an 8 passenger prop twin representative of this class of airplanes. The purpose of the RQAS is the reduction of vertical and lateral accelerations of the aircraft due to atmospheric turbulence by the application of active control. The current phase of the project includes the detailed design of the hardware, i.e. the airplane modifications, the Ride Quality Instrumentation System (RQIS), and the required computer algorithms. The aircraft modifications, consisting of the dedicated control surfaces and the hydraulic actuation system, have been designed at Cessna Aircraft under subcontract to KU-FRL. The instrumentation system, which consists of the sensor package, the flight computer, a Data Acquisition System (DAS), and the pilot and test engineer control panels, was designed by NASA LaRC. The overall system design and the design of the algorithms, both for flight control algorithms and ground system checkouts, were KU's responsibility. The system performance is predicted from linear simulation results and from power spectral densities of the airplane response to a Dryden gust. The results indicate that vertical acceleration (rms) reductions of 45% and lateral acceleration (rms) reductions of more than 50% are possible.

PRECEDING PAGE BLANK NOT FILMED

PAGE // INTENTIONALLY BLANK

Table of Contents

PRECEDING PAGE BLANK NOT FILMED

PAGE IV INTENTIONALLY BLANK

List of Figures

List of Tables

Nomenclature

A	system dynamics matrix
a	acceleration, ft/sec2
B	control effectiveness matrix
C	output matrix
C_L	lift coefficient
C_Y	side force coefficient
D	output matrix
g	gravitational acceleration, ft/sec^2
h	altitude, ft
J	cost function
K	gain matrix
L	scale length, ft
m	mass, slugs
p,q,r	angular rates, rad/sec
Q	state weighting matrix
R	control weighting matrix
S	reference wing area, ft^2
T	sample time, sec
t	time, sec
U	airplane speed, ft/sec
u,v,w	velocity components, ft/sec

$\mathbf{u}$	control vector
W	weight, lbs
$\mathbf{x}$	state vector
$\mathbf{y}$	output vector
α	angle of attack, rad
β	angle of sideslip, rad
Γ	control effectiveness matrix
δ_a	aileron deflection
δ_{df}	differential flap deflection
δ_e	elevator deflection
δ_f	flap deflection
δ_r	rudder deflection
δ_{se}	separate elevator deflection
θ	pitch angle, rad
σ	gust intensity, ft/sec
Φ	state transition matrix
Φ_g	power spectral density
ϕ	bank angle, deg
ω	frequency, rad/sec

Subscripts

1	trim state
a	aileron

b	body axes
df	differential flap
f	flap
e	elevator
g	gust
k	index
m	command model
p	pilot
r	rudder
se	separate surface elevator
x,y,z	coordinate axes
v	lateral
w	vertical

Special Notation

(′)	transpose
$( )^{ij}$	matrix element
(^)	estimated quantity

Acronyms

DAS	data acquisition system
KU-FRL	University of Kansas Flight Research Laboratory
NASA LaRC	NASA Langley Research Center
PI	parameter identification
PSD	power spectral density

RQAS	ride quality augmentation system
RQIS	ride quality instrumentation system

1. Introduction

Since the 1978 federal deregulation of the major air carriers, there has been an expansion in the smaller, commuter class air carriers into the routes that are not profitable for the larger carriers. With the renewed market for small (15 - 50 passengers) aircraft comes renewed interest in technological advances for small aircraft. While many new advances are being incorporated into existing aircraft and new designs, one area has received little attention, that of ride smoothing or ride quality. Due to the inherent characteristic of smaller aircraft, namely low wing loading, high aspect ratios and flight at low altitude, they are more susceptible to atmospheric gusts. This report summarizes the design of a Ride Quality Augmentation System (RQAS) performed by the University of Kansas Flight Research Laboratory (KU-FRL). RQAS is the implementation of an active digital flight control system for the expressed purpose of reducing aircraft vertical and lateral accelerations due to atmospheric turbulence. All of the research on the RQAS conducted at KU-FRL was done under the support and guidance of the NASA Langley Research Center.

The initial investigations which led to the current work involved a study of previous ride quality research and a feasibility study to determine the best approach to implementing an active digital control system (Reference 1). The first phase of the current work (Reference 2) began the theoretical design phase of a digital controller to be implemented on a Cessna 402B aircraft. This phase included the development of the Interactive Control Augmentation Design (ICAD) program which incorporates classical and optimal control design techniques along with several different analysis options into one package. Using the ICAD program, longitudinal RQAS controllers were designed and evaluated in batch simulations, on the KU-FRL hybrid simulator,

PRECEDING PAGE BLANK-NOT FILMED

and on the NASA Langley Research Center nonlinear real time simulator. The second phase of the project (Reference 3) continued the theoretical controller design. Several longitudinal and lateral controllers using different optimal control structures, output weighting and control rate weighting, were designed and evaluated. A preliminary design of the necessary aircraft modifications and an instrumentation system including the flight computer and the sensor package was also completed. The design of the aircraft modifications was done by Cessna Aircraft of Wichita, Kansas, under a subcontract to KU-FRL.

The current work, described in this report, constitutes the detailed design of both the RQAS hardware and software. The algorithms developed in the earlier phases have been refined. The hardware design has been completed in detail by the Cessna aircraft company to the desired specifications. An instrumentation system, consisting of the flight computer, the sensor package, a data recording system, and pilot and test engineer control panels has been designed by NASA LaRC and KU-FRL.

Chapter 2 of this report describes in detail the system philosophy and the general approach taken in the RQAS design. Chapter 3 then talks about the system functional design including a statement of the design goals and system requirements. It also states the final controller structure proposed for the system as well as projected system performance. The detailed system design is given in Chapter 4. This chapter includes the design of the control surfaces, the hydraulic system, the instrumentation system, and the flight software including failure detect algorithms. The proposed system operation is given in Chapter 5 and recommended future research in Chapter 6.

2. Problem Definition

A ride quality augmentation system (RQAS) is an active control system which improves passenger and flight crew comfort. This type of system is generally designed to reduce an aircraft's rigid body response to atmospheric turbulence. Although no standard criteria now exist for predicting comfort, mathematical models for passenger response to aircraft motion have been developed in which the dominant factors are the vertical and lateral accelerations (Reference 2).

In this chapter, the RQAS problem is defined. It is shown why small aircraft are more susceptible to gust than large transports. Then the objective and the design goals of the RQAS system are stated. Finally the basic approach used in the current research project is given.

2.1. Airplane Response to Turbulence

The main factors contributing to an airplane's sensitivity to gusts are its wing loading, W/S, and its lift curve slope, C_{L_α}. The relation between these parameters and the normal and lateral accelerations are given by Equations (2.1) and (2.2).

$$\bar{a}_z \propto C_{L_\alpha} \frac{\rho U_1}{W/S} \sigma_{g_w} \tag{2.1}$$

$$\bar{a}_y \propto C_{Y_\beta} \frac{\rho U_1}{W/S} \sigma_{g_v} \tag{2.2}$$

For commuter airplanes, W/S is low due to field length requirements, and C_{L_α} is high due to high-aspect-ratio wings with little sweep. In addition these airplanes

operate at low altitudes, where the gust intensities, σ_{gw} and σ_{gv} are high. The variation of gust intensity with altitude is shown in Figure 2.1 . All these factors combine to make commuter aircraft have higher levels of accelerations due to turbulence than large transports.

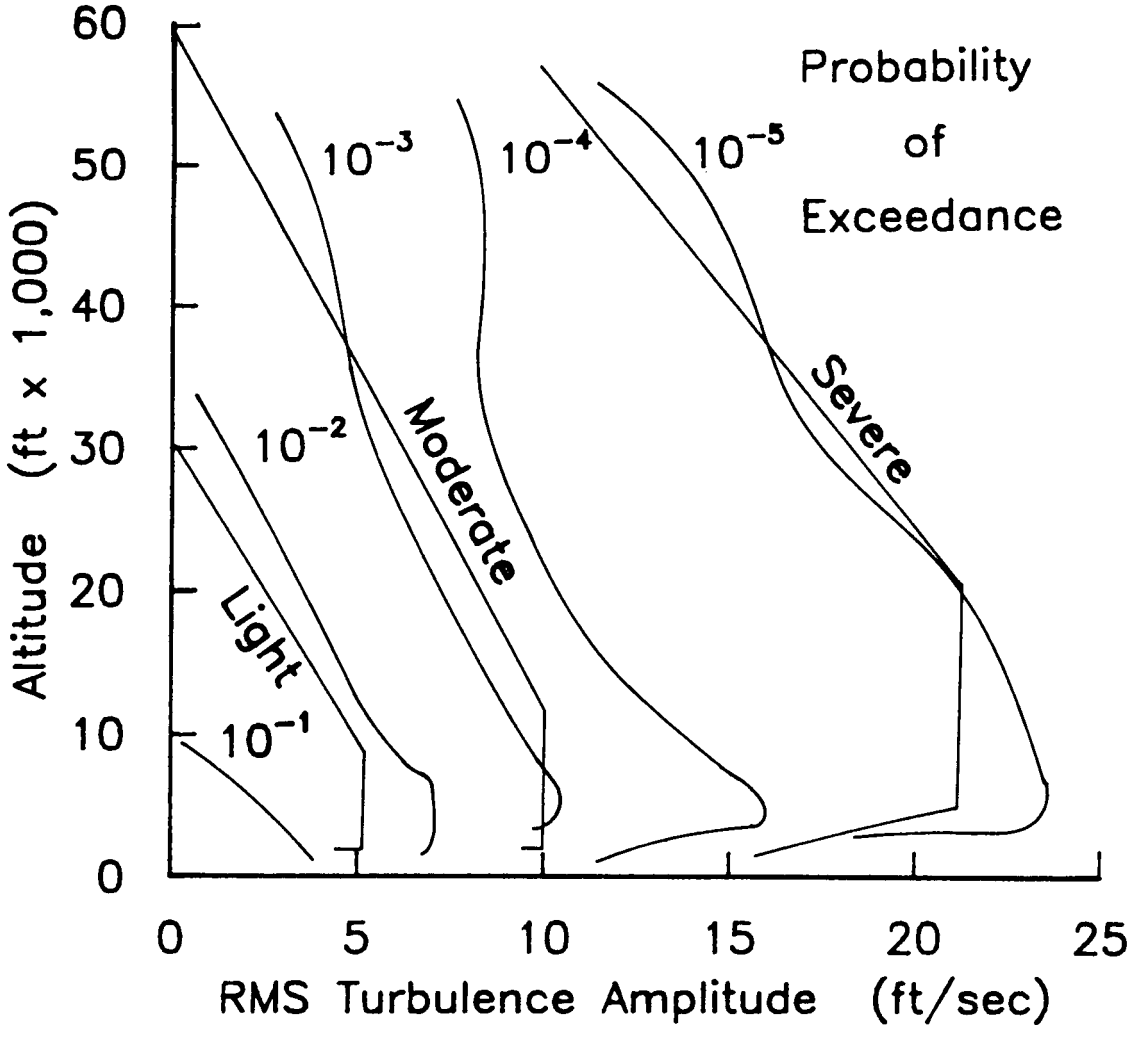

Figure 2.1 Variation of turbulence intensity with altitude (Reference 4)

As stated earlier, the perceived quality of the ride depends mainly on vertical and lateral accelerations. A comfort rating can be defined as (Reference 5):

$$C = 2.1 + 17.2\,\bar{a}_z + 17.1\,\bar{a}_y \tag{2.3}$$

where $\bar{a}_z$ = rms vertical acceleration

$\bar{a}_y$ = rms lateral acceleration

This comfort rating corresponds to passenger satisfaction as determined by actual passenger surveys. A comfort rating of 4, for example, means that 80% of the passengers will be satisfied with the ride; a rating of 7 corresponds to only 25% passenger satisfaction.

Figure 2.2 shows the comfort rating of an open loop Cessna 402B, i.e. without RQAS, over a typical mission flight envelope. It is obvious that for moderate turbulence (probability of exceedance = 10^{-3}) only a small percentage of passengers will be satisfied with the ride.

2.2 RQAS Objective and Design Criteria

The RQAS project is a research program whose objective is to evaluate the use of an active digital control system for gust alleviation. The RQAS is to be evaluated both theoretical by means of frequency response and time response analysis as well as through flight tests. The theoretical performance evaluations have been done at the KU-FRL and the results will be summarized in Chapter 4. The flight tests are to be performed with a modified Cessna 402B airplane. This airplane will provide a low cost test bed, which can also be used in the future for other stability augmentation research.

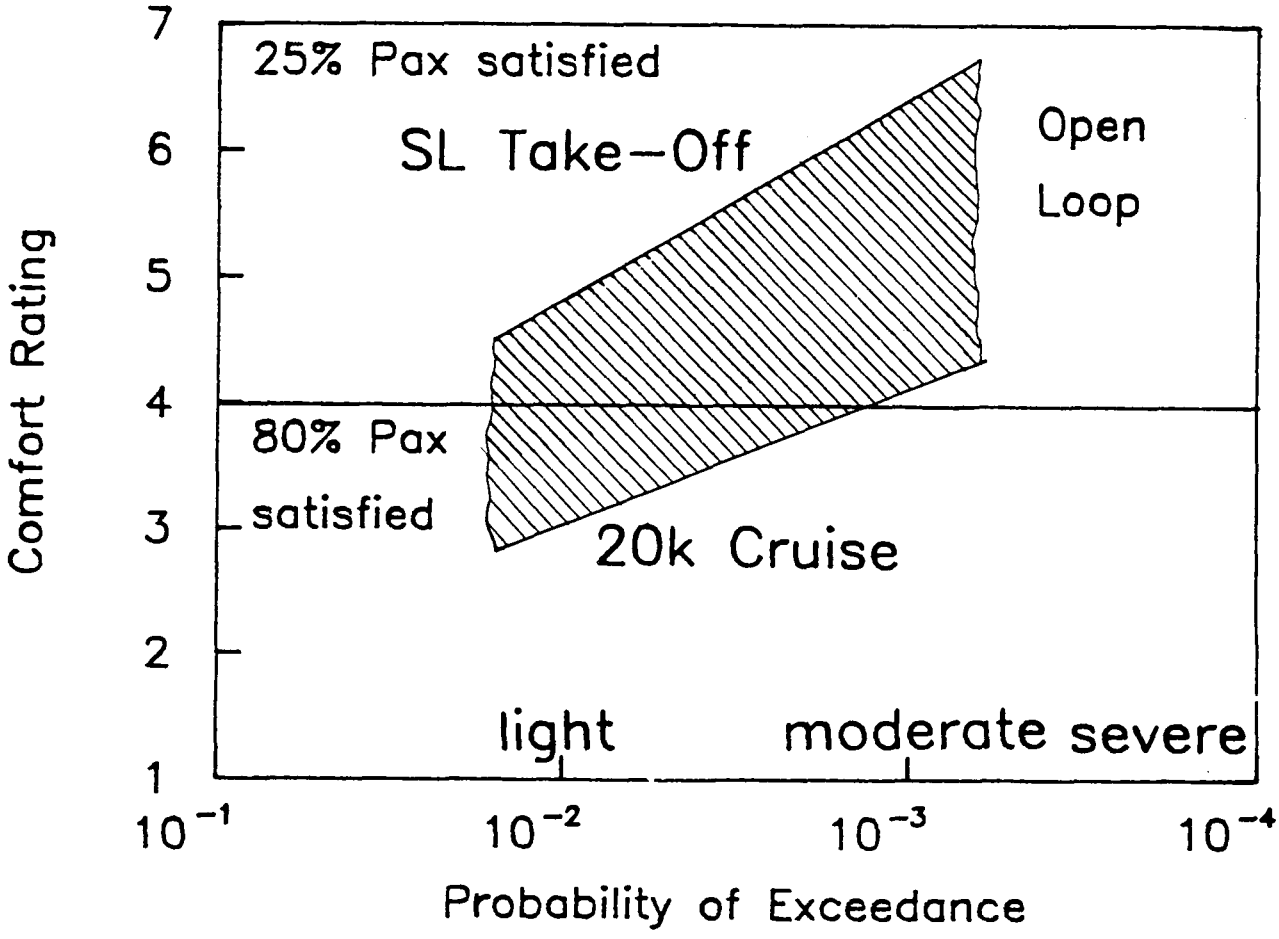

Figure 2.2 Comfort Rating for Cessna 402B

2.2.1. Design Goals

The design goals for the RQAS project have been established based on the surveys mentioned in Section 2.1. If we want to achieve a comfort rating of 4, i.e. 80% of the passengers are satisfied with the ride, and we realize that the vertical rms acceleration is much larger than the lateral rms acceleration, Equation (2.3) gives a value of 0.11 g or 3.54 ft/sec^2 for $\bar{a}_z$. This value of 0.11 g has also been used as the upper limit for acceptable vertical rms accelerations in a BOEING STOL ride quality

augmentation study, Reference 6. In this case the value was established based on moving base simulator results. The design goal is marked on Figure 2.2. Note that the unaugmented airplane shows a much lower comfort rating than 4 for most of its flight envelope. For the other vehicle motions no design guidelines exist so that for the present study any reduction of the unaugmented vehicle motion is desirable.

In addition to the performance goals there are certain design constraints. The control surface travel will be limited to practically feasible values. During the design of the test vehicle a further reduction in the maximum available outboard flap deflection was required to provide safe operation. This will be discussed in Section 3.1. Flap rate limits were selected as values that were technically and economically feasible. All these design criteria are summarized in Table 2.1.

2.3 General Approach

The RQAS system is designed as a digital control system capable of creating forces and moments in all three axes. It uses dedicated control surfaces for direct-lift, pitching moment, and roll control, and the full rudder for yaw control. Figure 2.3 shows the airplane with these dedicated control surfaces. Direct-lift and roll control are achieved through modified flaps, which can now move up and down. These flaps extend over the wing trailing edge to provide enough surface area. The original split flaps were partly underneath the nacelle, but this part could not be used because of the great difficulty in predicting flap moment coefficients with the nacelle covering a part of the flap. The outboard portion is used as a flaperon, i.e. differential deflection of this part of the flaps is used for roll control. A separate surface elevator is used for pitch control. Since the RQAS system does not need a large pitch control authority,

Table 2.1 RQAS Design Criteria

Longitudinal

Variable	Criterion
a_z (rms)	< 3.54 (ft/sec^2)
α, u, q, θ	as close to open loop as possible
$\lvert\delta_f\rvert$	< 8 (deg) safety limit for outboard flaps < 20 (deg) physical limit for all flaps
$\lvert\delta_{se}\rvert$	< 10 (deg)
$\dot{\delta}_f$	< 120 (deg/sec)
$\dot{\delta}_{se}$	< 50 (deg/sec)

Lateral

Variable	Criterion
a_y	< 50% of open loop
p, r	any reduction is desirable
β, ϕ	as close to open loop as possible
$\lvert\delta_{df}\rvert$	< 8 (deg) safety limit for outboard flaps
$\lvert\delta_r\rvert$	< 10 (deg)
$\dot{\delta}_{df}$	< 120 (deg/sec)
$\dot{\delta}_r$	< 20 (deg/sec)

the small separate surface elevator is sufficient for this purpose. The entire airplane rudder is used for yaw control. This was necessary, because the airplane needs the entire rudder in an engine-out situation, and therefore no portion of it could be used as a separate surfaces. Other options, for example a ventral fin, were investigated in

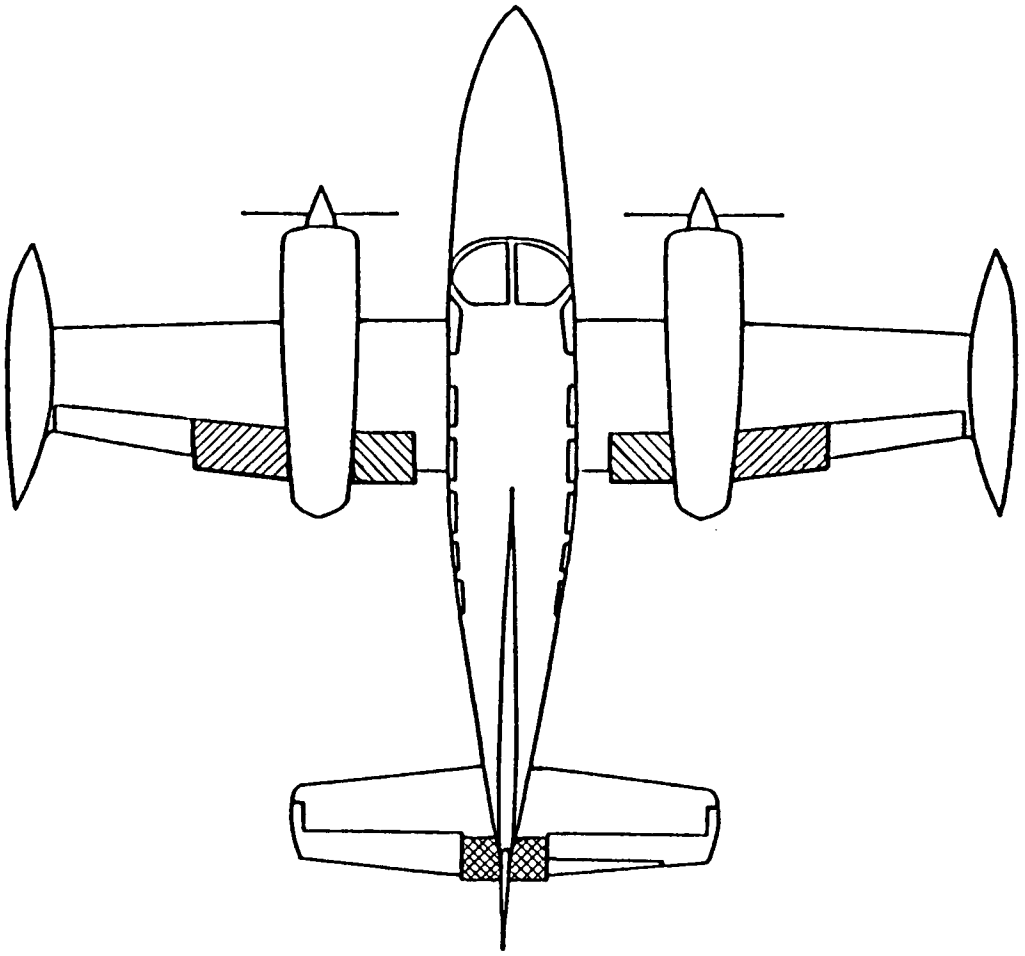

Figure 2.3 Cessna 402B Research Aircraft

Phase one of this project (Reference 3) but were found to be not feasible. To drive the rudder a standard autopilot servo is used. This provides the pilot with a simple override capability, since he can always overpower the slip-clutch. In normal research flight operation, however, the pilot is instructed not to use the rudder, since the RQAS uses it for lateral control.

The complete RQAS system consists of the modified airplane, the Ride Quality Instrumentation System (RQIS), the RQAS software, a test engineer's station, and a pilot control panel. The RQIS incorporates the computer, a sensor package, and a data recorder. The functional layout of the system is shown in Figure 2.4. The flight

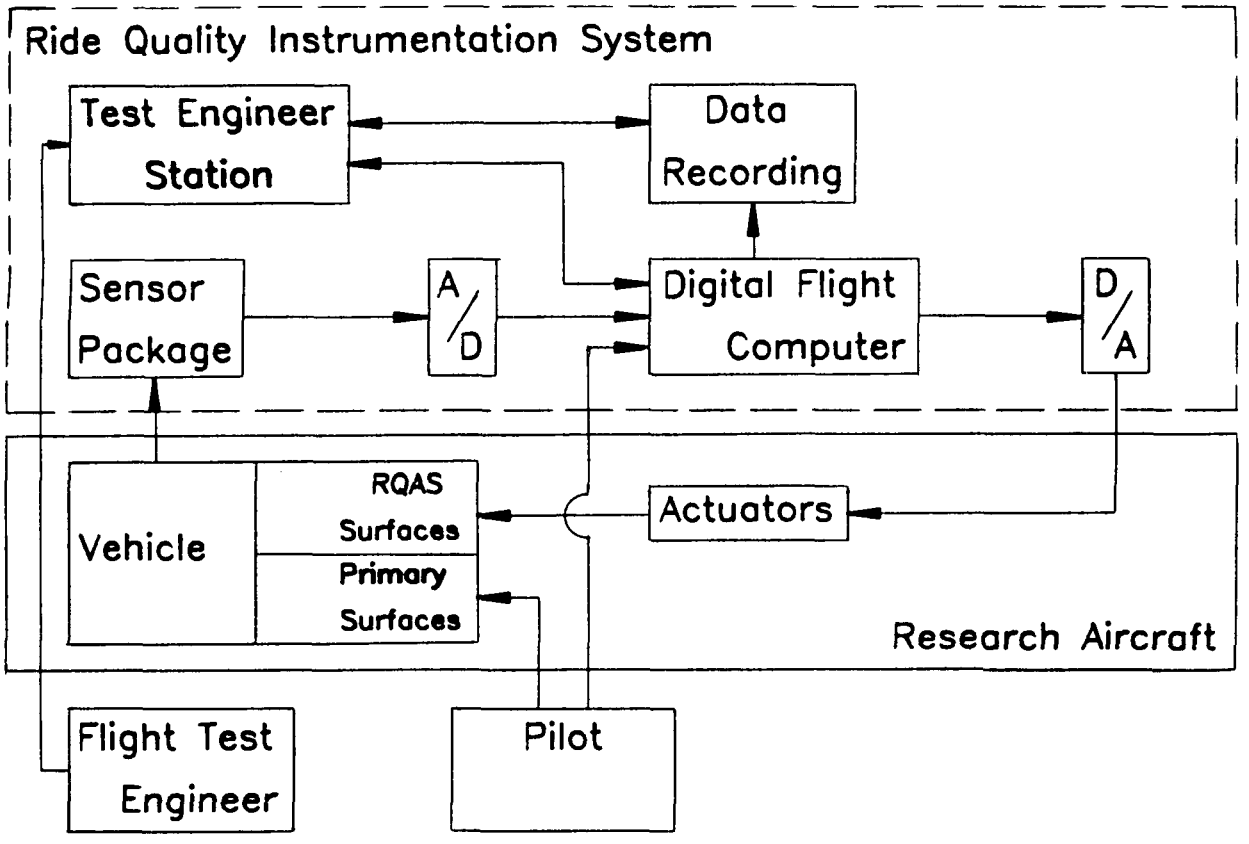

Figure 2.4 RQAS Experimental System

computer uses the data from the sensor package to recognize airplane accelerations due to turbulence and moves the RQAS control surfaces according to the implemented control law to counter those accelerations. All sensor data plus some computed variables are recorded for documentation and post flight analysis. The RQAS system

can be operated from two control panels, one on the test engineer station, and the other on the pilot instrument panel. The latter has only limited capabilities, but is sufficient for operation of the system for demonstration flights.

2.4 Basic Equations

The RQAS control laws were designed using variations of the optimal linear quadratic regulator. The fundamental assumption in applying these techniques is that the aircraft dynamics about a trim point can be described by a set of linear first-order differential equations in a state matrix form;

$$\dot{\mathbf{x}} = \mathbf{A}\mathbf{x} + \mathbf{B}\mathbf{u} \quad , \tag{2.4}$$

where $\mathbf{x}$ is the aircraft state vector, $\mathbf{u}$ is the control vector and the matrices $\mathbf{A}$ and $\mathbf{B}$ are constant coefficient matrices. The longitudinal and the lateral-directional equations have been separated, so that

$$\mathbf{x}'_{long} = [\alpha \; u \; q \; \theta], \qquad \mathbf{u}'_{long} = [\delta_{se} \; \delta_f],$$

$$\mathbf{x}'_{lat} = [\beta \; p \; r \; \phi], \qquad \mathbf{u}'_{lat} = [\delta_{df} \; \delta_r].$$

The coefficients of the system dynamics matrix, $\mathbf{A}$, and the control effectiveness matrix, $\mathbf{B}$, are found as linearizations at a trim flight condition of a non-linear six degree-of-freedom simulation model of the Cessna 402B existing at NASA LaRC. Models of the airplane were generated at five different trim flight conditions, which were selected to represent a typical mission flight envelope. These flight conditions are listed in Table 2.2. The $\mathbf{A}$ and $\mathbf{B}$ coefficient matrices are listed in Appendix A. A

Table 2.2 RQAS Trim Flight Conditions

Flight Condition		Altitude	Speed
I	Takeoff	S.L.	184 ft/sec
II	Climb	S.L.	211 ft/sec
III	Climb	5,000 ft	227 ft/sec
IV	Cruise	20,000 ft	358 ft/sec
V	Approach	S.L.	182 ft/sec

derivation of the airplane equations of motion and their transformation into state variable form can be found in Reference 7.

Since the controller is implemented in a digital computer, the sampled data regulator approach is used. The controls, $\mathbf{u}$, are held constant over each sample interval, and the problem is formulated as follows: Find the control sequence $\mathbf{u}_k$, k = 0,1..., that will minimize the continuous time cost function for the selected regulator formulation. Two different formulations are used for the RQAS system, output weighting and control rate weighting. Output weighting allows variables, which are a linear combination of states and controls, to be directly weighted in the cost function. The continuous time cost function for the output weighting case is:

$$J = \frac{1}{2} \int_0^\infty (\mathbf{y}'\mathbf{Q}\,\mathbf{y} + \mathbf{u}_k'\mathbf{R}\,\mathbf{u}_k)\ dt \qquad (2.5)$$

Control rate weighting allows the control rates to be directly weighted in the cost function in order to avoid excessive control rates. In this case the continuous time cost function is given by:

$$J = \frac{1}{2} \int_0^\infty (\mathbf{y}'\mathbf{Q}\,\mathbf{y} + \mathbf{u}_k'\mathbf{R}\,\mathbf{u}_k + \dot{\mathbf{u}}_k'\mathbf{M}\,\dot{\mathbf{u}}_k)\ dt \tag{2.6}$$

For the present application the output vector is

$$\mathbf{y}_{long}' = [a_z\ a_x\ \alpha\ \ u\ \ q\ \ \theta], \tag{2.7}$$

$$\mathbf{y}_{lat}' = [a_y\ \beta\ \ p\ \ r\ \ \phi].$$

Q, **R**, and **M** are weighting matrices which are chosen to be diagonal. The elements of these matrices reflect the relative importance of the outputs or controls by weighting those variables in the cost function integral. For a solution to exist, **Q** must be positive semi-definite and **R** must be positive definite.

Using the output vector **y** in the cost function allows the control designer to directly weight quantities that are given as a linear combination of states and controls. This is especially useful for a ride quality augmentation system, because the variables of primary interest, i.e. the accelerations, can be expressed in this manner, e.g.,

$$a_z = U_1\dot{\alpha} - U_1\cos(\alpha_1)q + g\sin(\theta_1)\theta \tag{2.8}$$

Note that $\dot{\alpha}$ can be replaced by the first state equation (2.4) and hence:

$$a_z = [U_1A_{11} \quad U_1A_{12} \quad U_1(A_{13}-\cos\alpha_1) \quad U_1A_{14}+g\sin\theta_1] \begin{bmatrix} \alpha \\ u \\ q \\ \theta \end{bmatrix} \qquad (2.9)$$

$$+ [U_1B_{11} \quad U_1B_{12}] \begin{bmatrix} \delta_{se} \\ \delta_f \end{bmatrix}$$

Therefore a_z represents an element of the output vector **y**.

3 System Implementation And Detailed Design

This chapter describes in detail the implementation and the components of the RQAS system. As mentioned in Section 2.3, the system consists of the Cessna 402 airplane with modified control surfaces, a hydraulic actuation system, an instrumentation system, and the flight software.

Section 3.1 addresses the influences of safety related issues on the system design. The overall design of the RQAS system was done by KU-FRL. This overall design also includes the design specifications for the various components. The mechanical airplane modifications as well as the hydraulic system have been designed in detail by Cessna Aircraft under subcontract to KU-FRL. A complete set of drawings is on file both at Cessna Aircraft and at KU-FRL. The airplane modifications are described in Section 3.2. The Ride Quality Instrumentation System (RQIS) has been designed at NASA-LaRC. Its various components are described in Section 3.3. The overall RQAS wiring, excluding the sensor package and the data recording system, is presented in Section 3.4, including the interconnections between the various components. KU-FRL has developed both the flight software and the checkout procedures. These are outlined in Section 3.5.

3.1 Safety Considerations

An important concern in any flight test is safety. The philosophy used in RQAS design to ensure safety is that no failure that may occur can be catastrophic. This is achieved by limited control authority for the RQAS control surfaces. Thus even in the case of control surfaces jammed at their hardover position the pilot has sufficient

control authority in the standard aileron and elevator control surfaces to safely land the airplane. The validity of this concept has been verified by piloted simulations using the NASA LaRC General Aviation Simulator in August 1987. For this purpose the flight control laws developed in the earlier phase of the project (Reference 3) were programmed into the simulator and a variety of possible failure situations were simulated, including the most hazardous one, a differential hardover failure of the outboard flaps. One result of the study is that no failure posed any safety problem if the system could be disengaged, either automatically or by the pilot. If the system could not be disengaged, or if the control surfaces were mechanically jammed, only the case of the differential flap failure was found to be potentially dangerous. It was found that in this worst case the outboard flap travel should be limited to 8 degrees, so that the pilot would have enough control power with the ailerons to overpower the differential flap deflection. This restriction was incorporated in the recommended design.

The RQAS design includes several other features to enhance the safety of flight test operation. One such feature is the installation of a centering and locking mechanism for the RQAS control surface. This mechanism ensures that the dedicated control surfaces are fixed in there zero deflection condition after the system is disengaged. The system can be disengaged manually by either the pilot or the test engineer. In addition, an automatic disengage can be triggered in several ways. The flight software includes algorithms that detect error conditions such as faulty sensor signals, the airplane leaving the operational envelope of the RQAS, or control commands larger than the allowed deflection limits. In addition mechanical limit switches on the control surfaces ensure an automatic disengage in case of control surface hardovers even if for some reason this condition has not been detected by the

software. A disengage, either manual or automatic, will turn off the hydraulic power and activate the locking mechanism, thereby returning the airplane to its original configuration.

3.2. Control System Mechanical Design

The mechanical design of the control system, i.e. the design of the control surfaces, hydraulic system, and actuation system, was done at Cessna Aircraft under subcontract to KU-FRL. An overview of the airplane modifications, showing the location of all components, is given in Figure 3.1. The control system is designed such that the normal operational envelope of the airplane is retained with the system "OFF". In the current design, the pilot will have no control over the flaps, and hence the airplane is landed with the flaps locked in the neutral position. The operational envelope with the RQAS "ON" will be determined by static load or flutter analysis to be performed during the vehicle modification. The RQAS control surfaces were designed to ultimate hinge moments of 1.5 times the limit loads determined by Cessna Aircraft. These limit loads are listed in Table 3.1. The control surfaces and the

Table 3.1 Control Surface Maximum Hinge Moments

Control Surface	Max. Hinge Moment[1] (in-lbs)
Separate Surface Elevator	553
Flap (inboard)	3,488
Flap (outboard)	4,429

[1] These are limit loads. The control surfaces are designed for these loads multiplied with a design safety factor of 1.5.

ORIGINAL PAGE IS
OF POOR QUALITY

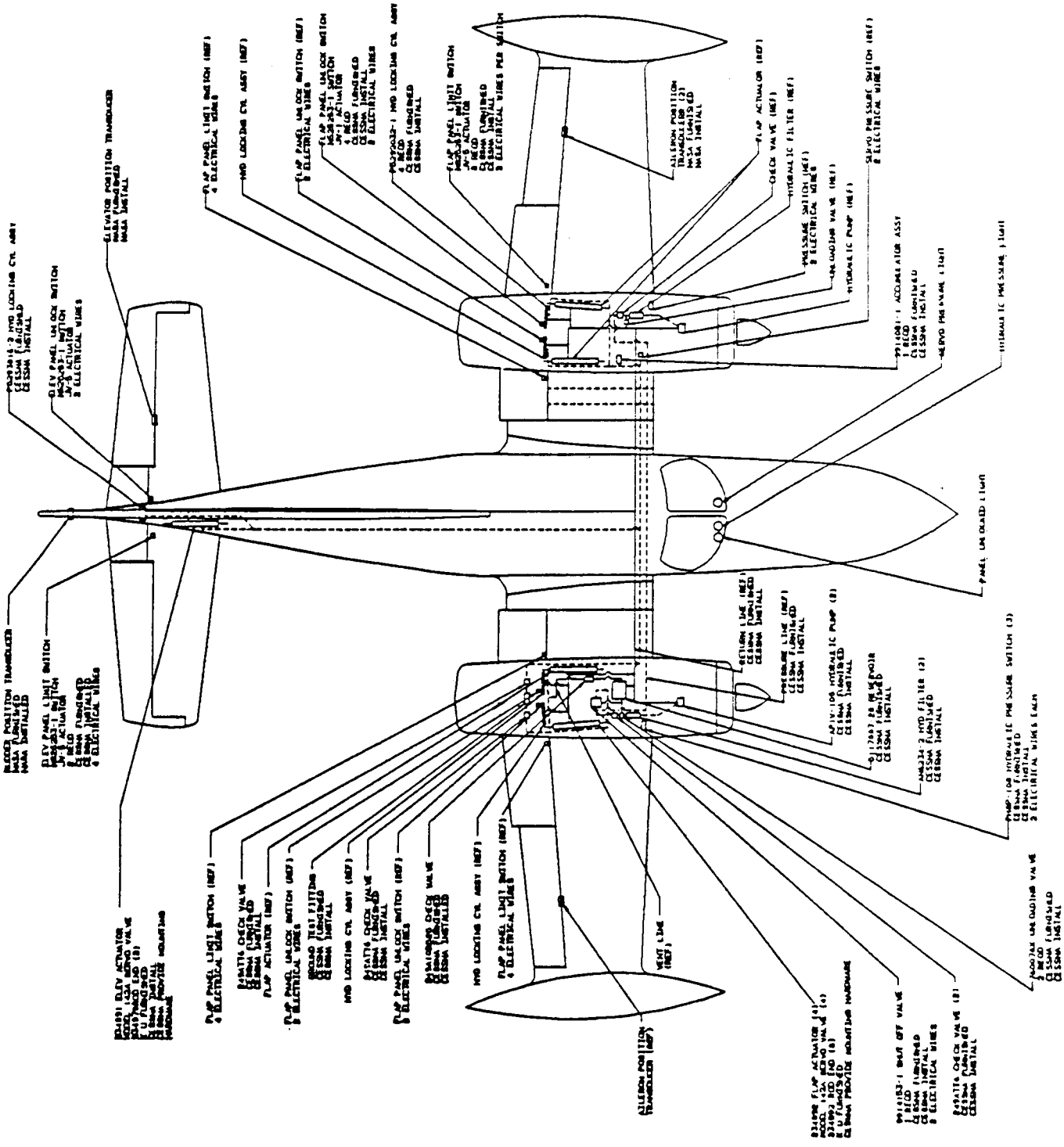

Figure 3.1 System Modifications Overview (Cessna Aircraft)

actuation system were designed to provide maximum deflections and rates as specified in Table 2.1.

3.2.1. Control Surfaces

A view of the modified airplane was shown in Figure 2.3. The shaded areas are the RQAS control surfaces. The following sections will discuss the design of each of these surfaces. All drawings were provided by Cessna Aircraft.

3.2.1.1. Flaps and Nacelle

The split flap of the airplane will be replaced by a plain flap using the same flap attachment hinge, so that no modification of the primary wing structure is necessary. Figure 3.2 shows the geometry of both the inboard and outboard flaps. Note that the chord of the flaps has been increased, so that the flaps now extend over the wing trailing edge. This was necessary to compensate for the loss of flap area under the nacelle. Using the area under the nacelle would have required both modification of the nacelle locker to provide for upward flap travel, and an estimate of the aerodynamic interference between flap and nacelle, which would have been impossible to predict.

The flaps are an all metal conventional design (industry standard). They are hinged with a piano hinge at the lower surface, so that the existing hinge line of the old split flaps could be used. The mechanical design permits a maximum deflection of 20 degrees in either the up or down direction. The basic design of an inboard flap is

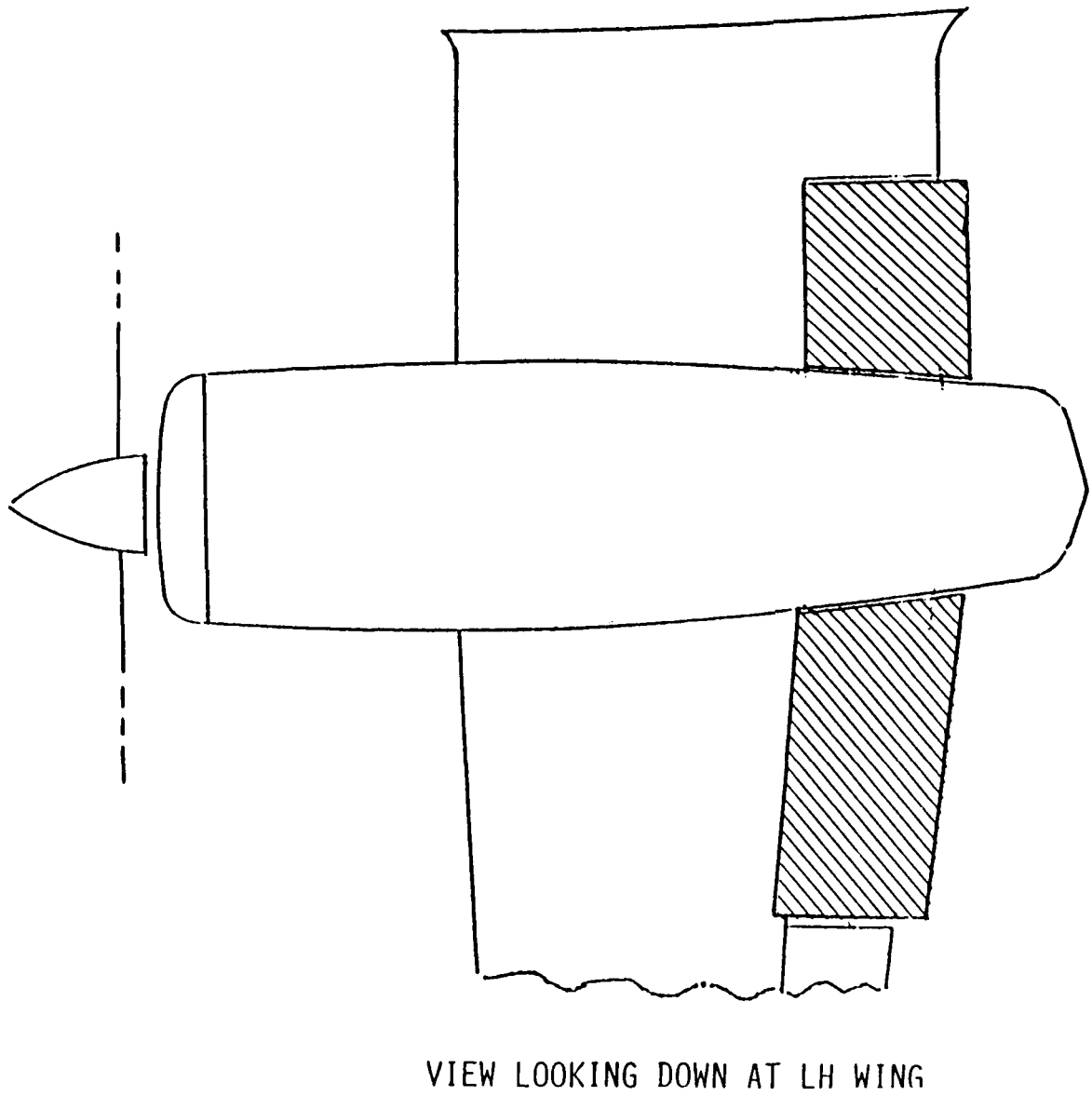

Figure 3.2 Flap Geometry (Cessna Aircraft)

shown in Figure 3.3. A closure plate is required on the nacelle to cover the area previously covered by wing structure.

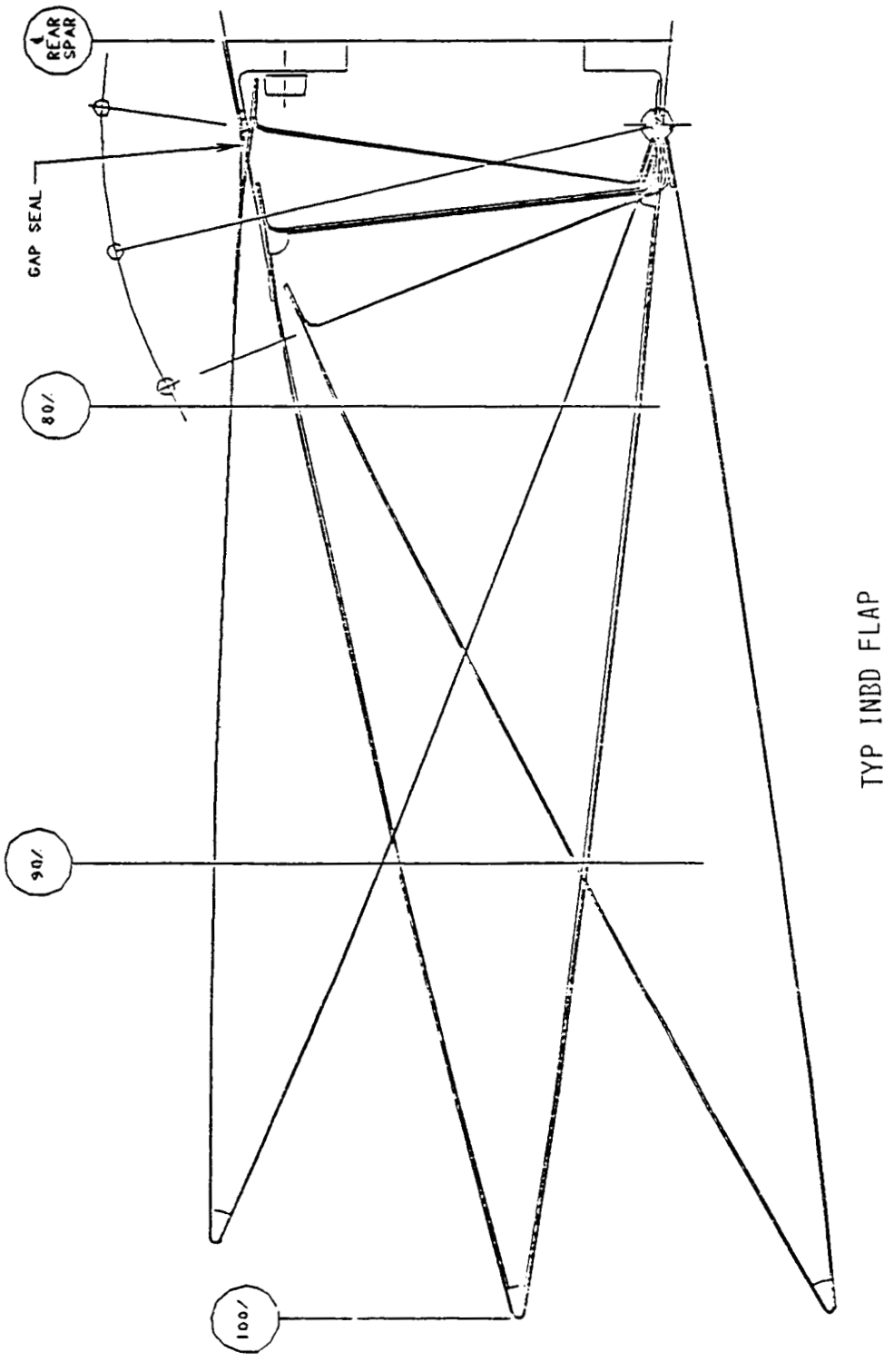

Figure 3.3 Inboard Flap (Cessna Aircraft)

3.2.1.2. Separate Surface Elevator

The separate surface elevator, shown in Figure 3.4, is a rather small control surface, which is placed in a currently fixed area of the horizontal stabilizer. It is designed for ±10 degree deflection and both the left and the right surface have a common torque tube with a single actuator. The separate surface elevator is also designed in all metal construction, and no change to the primary elevator control system is necessary.

3.2.1.3. Rudder

Since the entire rudder is used for RQAS purposes, no separate control surfaces is needed. The rudder will be driven by a standard autopilot servo , a King Radio KS 271. Although the full rudder will be driven a minor modification of the rudder is necessary to avoid mechanical interference with the separate surface elevator. A small piece of the rudder trim tab needs to be cut off to allow for an upward deflection of the elevator. Figure 3.5 shows this modification.

3.2.2. Hydraulic System

The hydraulic system is designed as a full time system with a design pressure of 2050 psi. A schematic diagram is shown in Figure 3.6. There is one pump on each engine, and both pumps are operating permanently. The pumps selected for the system are standard pumps, Abex P/N APIV-105, which are used on the Cessna

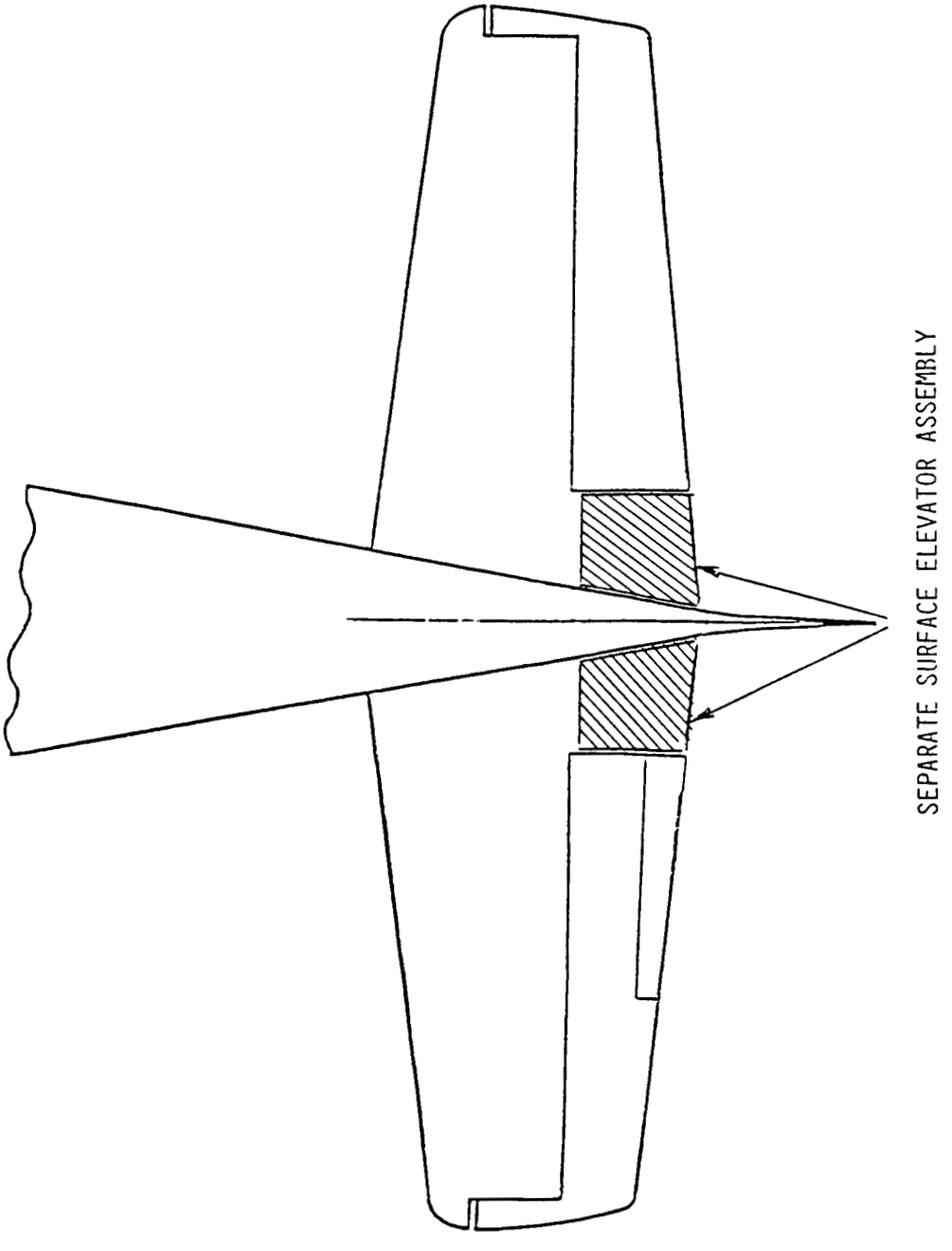

Figure 3.4 Separate Surface Elevator (Cessna Aircraft)

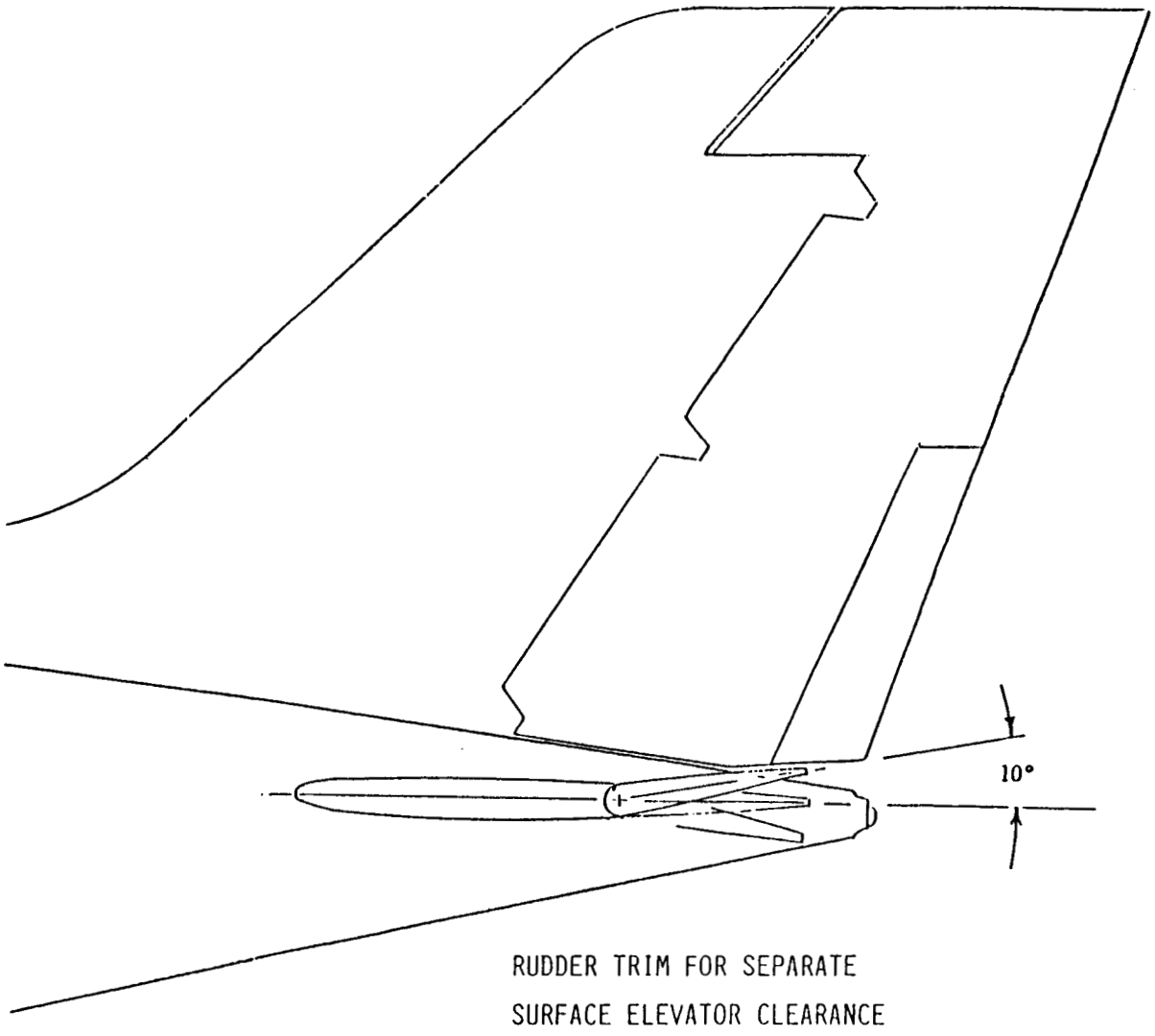

Figure 3.5 Rudder Trim Tab Modification (Cessna Aircraft)

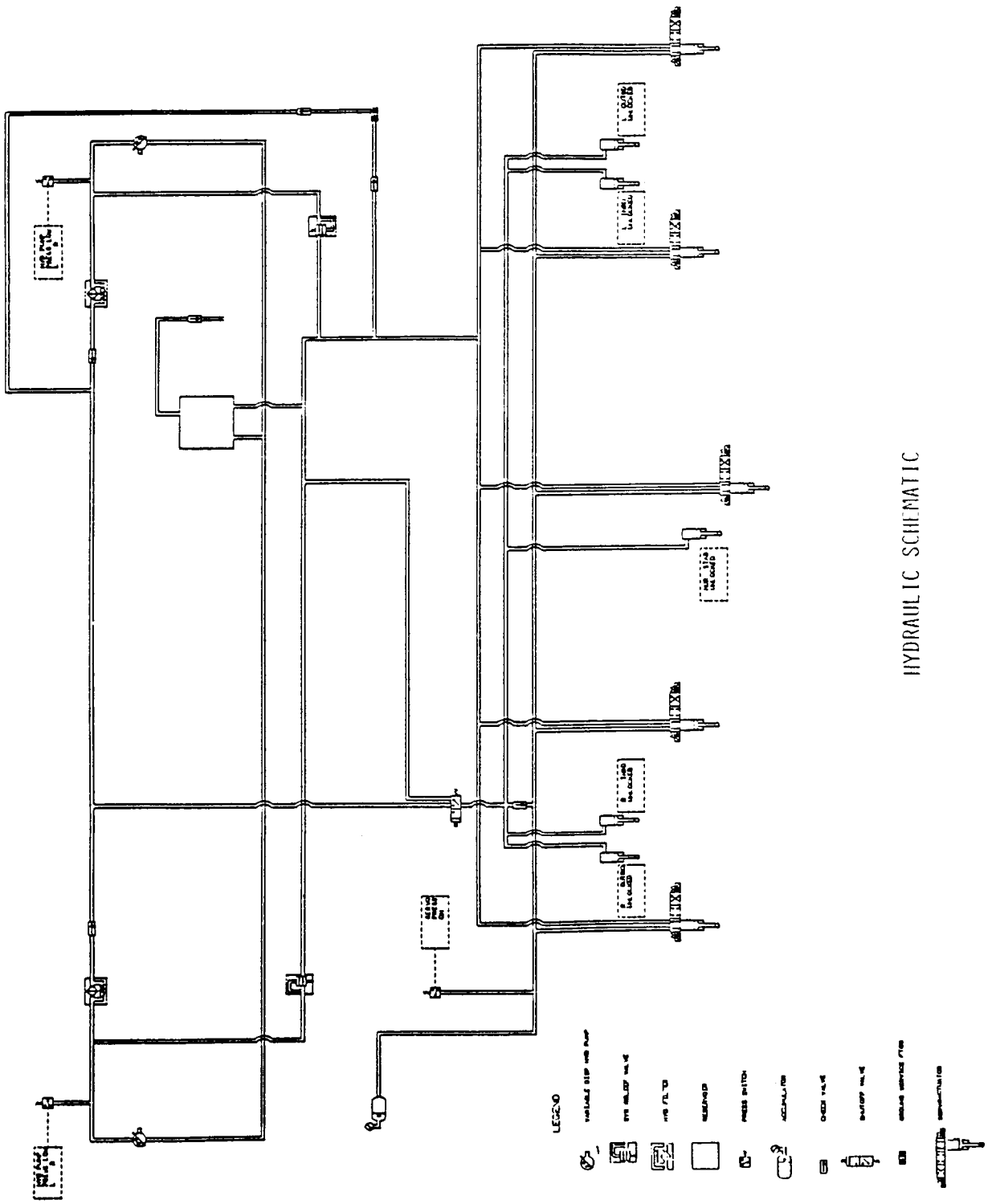

Figure 3.6 Hydraulic System (Cessna Aircraft)

Citation III aircraft. They provide 3 gpm at 3450 rpm each and a single pump can operate the system, but not provide the maximum design control surface deflection rates. One hydraulic reservoir is used and mounted in the right wing locker. It has a capacity of 76 in^3. Hydraulic filters are provided for each pump, as well as a relief valve for pump malfunction. Pressure switches to indicate low pressure are installed on both pumps and after the shut-off valve. The shut-off valve separates the actuators from the pumps when the hydraulic system is disengaged. An accumulator , Cessna P/N 9914081-1 - Teledyne Sprague P/N 60000-1, is provided as a system damper and to improve actuator response. It also provides hydraulic pressure to center the control surfaces after the system has been disengaged. Special locking actuators, Cessna P/N P5292032-1, which are shown in Figure 3.7, are installed to lock the control surfaces in the neutral position when the system is "OFF". These actuators are spring loaded and retract a pin when hydraulic pressure is applied. Therefore, loss of pressure causes the pins to extend, and as the control surfaces reach zero deflection the pins move into tapered holes in the surfaces and lock them in place.

3.2.3 Actuators

The RQAS uses linear hydraulic actuators to operate the control surfaces. The actuator type selected for this application are Schenck Pegasus 1.1 KIP actuators with a model 142A servo valve. This actuator provides an output load of 600 lbs at the system operating pressure of 2050 psi and is fatigue rated. It is manufactured with various stroke lengths. A 4 in stroke is used for the separate surface elevator, providing ±10 degrees of deflection. A 6 in stroke is used for the inboard flaps, which have a ±20 degree deflection range. Two options exist for the outboard flaps, whose

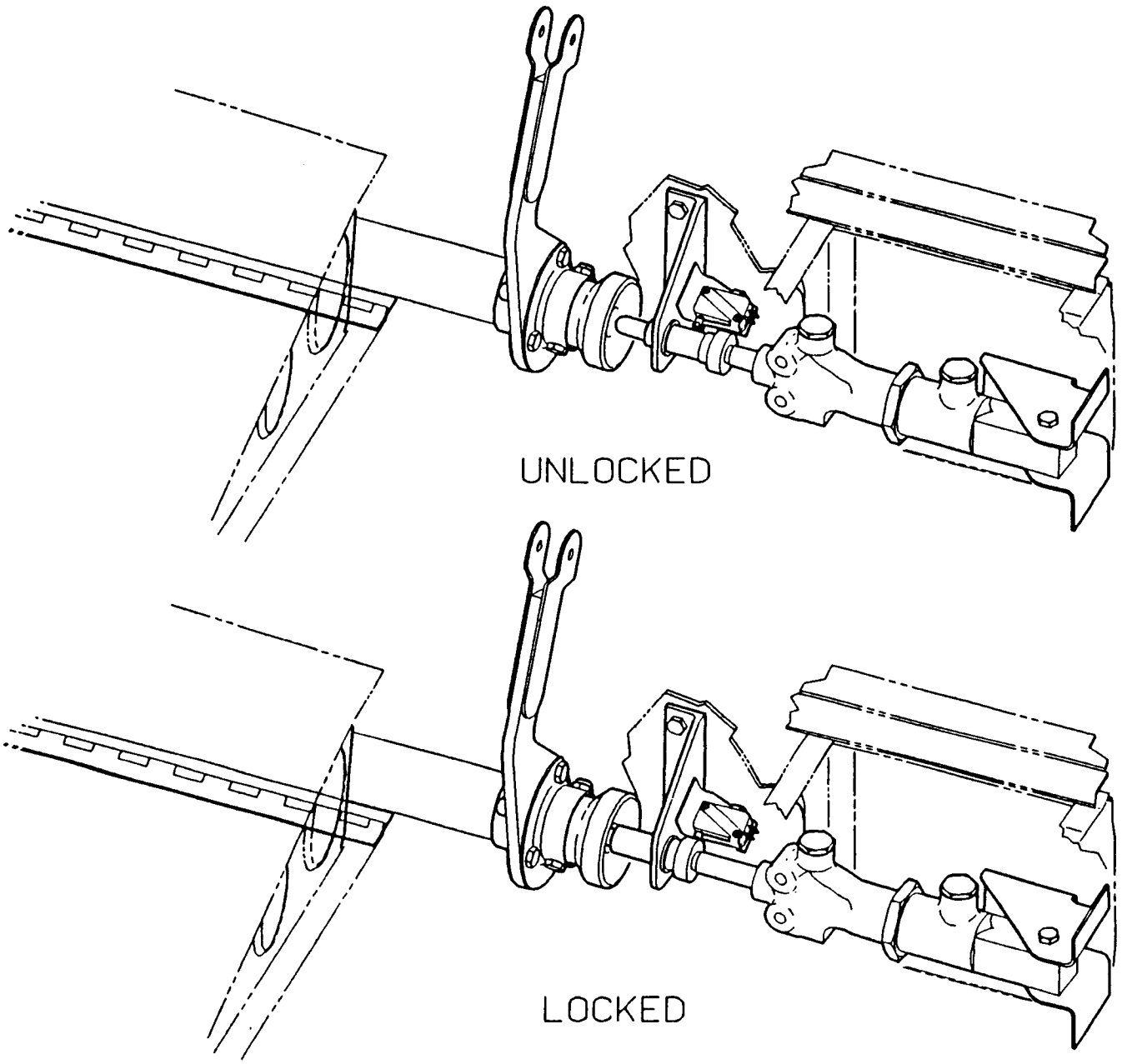

Figure 3.7 Locking Mechanism (Cessna Aircraft)

maximum range is limited to ±8 degrees for safety reasons. The first option is to use a custom manufactured actuator with a stroke of 2.4 in. The second option is to use a standard actuator and limit its stroke by internal modification. An LVDT is used for position feedback. Special electronic drive modules, SSM1, are also available from Pegasus for the actuators. These drive modules are being examined by NASA for use in the system.

These actuators are generally used in ground testing equipment and were found to be strong and fast enough for the RQAS system, however, they are not flight certified. Therefore NASA LaRC is conducting flight qualification tests on a sample actuator.

The flap actuators are installed in the wing locker as shown in Figure 3.8. The elevator actuator is installed in a special fairing underneath the fuselage. Figure 3.9 shows the installation of this actuator.

3.3 Ride Quality Instrumentation System

The Ride Quality Instrumentation system contains the flight computer, the sensor package, a data recording system, and the test engineer's and pilot's control panel. The system is installed on two pallets for quick installation into the airplane. These pallets will be mounted in the fuselage near the c.g., replacing the passenger seats. The data recorder is installed in the luggage compartment in the nose of the airplane. The installation is shown in Figure 3.10.

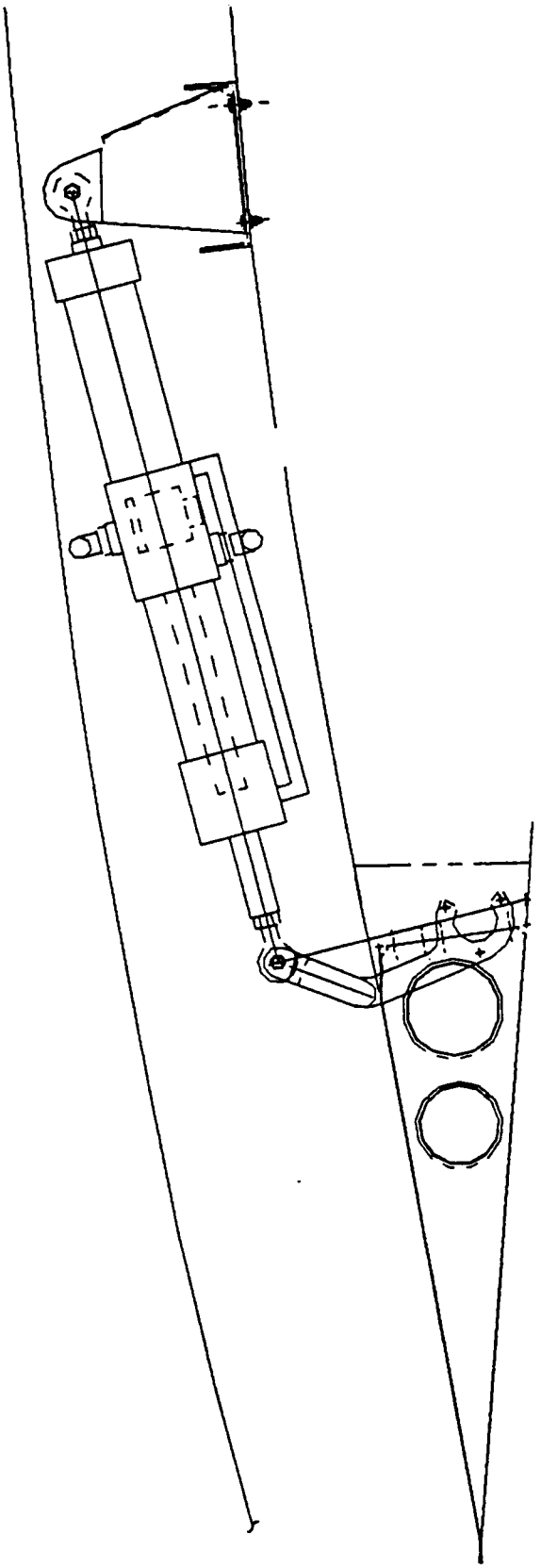

Figure 3.8 Flap Actuator Installation (Cessna Aircraft)

ORIGINAL PAGE IS
OF POOR QUALITY

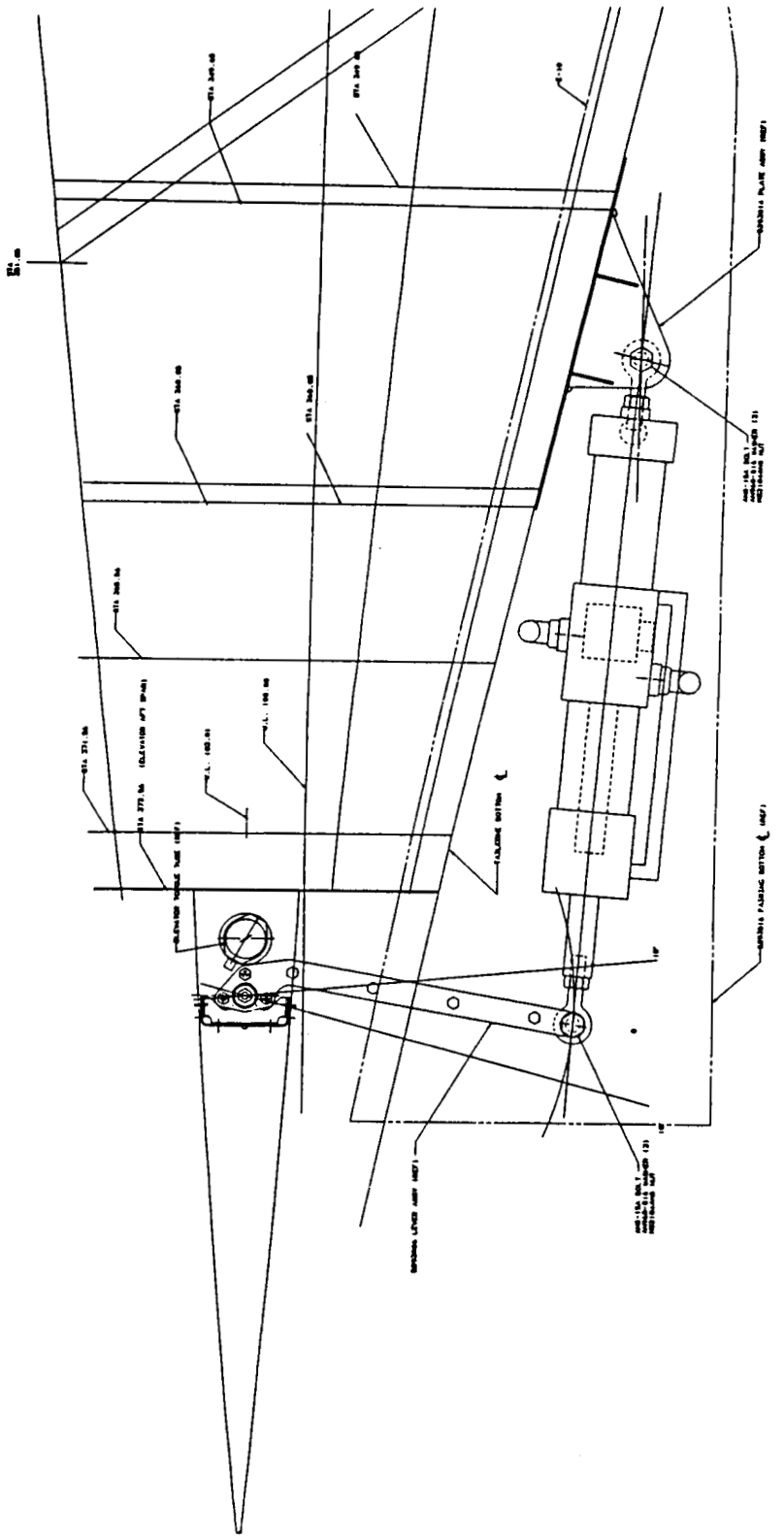

Figure 3.9 Elevator Actuation (Cessna Aircraft)

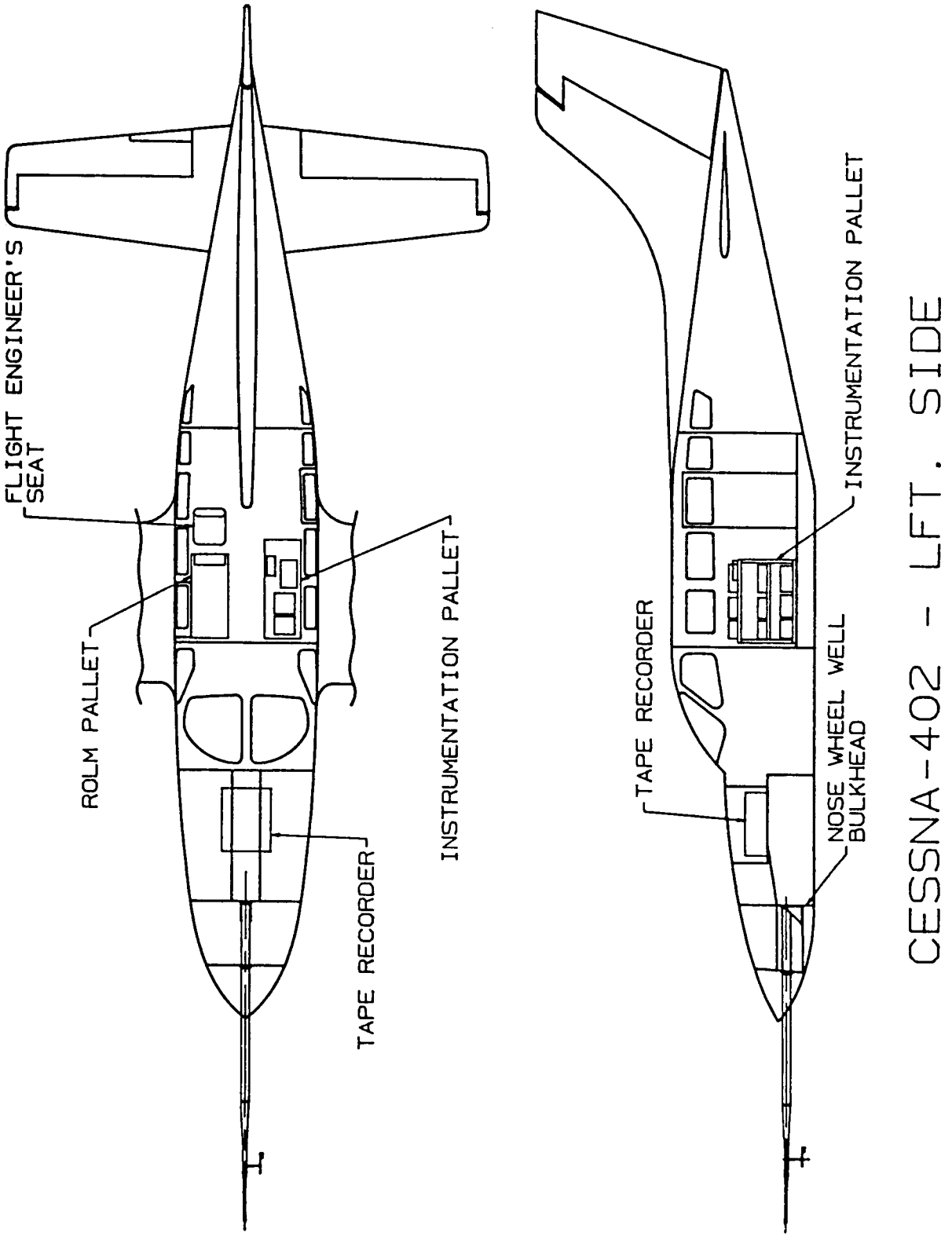

Figure 3.10 RQIS Installation (NASA LaRC)

3.3.1 Flight Computer

The flight computer mechanizes the control algorithms of the RQAS system. It also performs checks on the input and output data and automatically issues a disengage signal in the case of unreasonable data values. The computer selected for the system is a ROLM 1666B. A functional block diagram of the Rolm computer system is shown in Figure 3.11. This computer is a powerful flight certified machine with high level language (FORTRAN) support. The FORTRAN language makes development of the flight software easy, since it is easy to program and the software can be tested out on other computers before being installed in the actual flight computer. The ROLM can be controlled from its own control panel and also from a handheld terminal, which is connected to the computer via a standard serial interface. This terminal allows the test engineer to run the RQAS software, set program parameters and check specified memory locations.

The computer is equipped with a set of A/D and D/A boards to interface with the analog sensors and actuator drive electronics. These converters have an analog range of ±10V. In addition to the flight hardware, a ground support system is also available. This system includes a terminal, a disk subsystem, and a printer. The disk subsystem is used to load the flight software into the computer before take-off. The terminal is used to download the flight data from the on-board data recording system to hard disk and for data reduction and plotting.

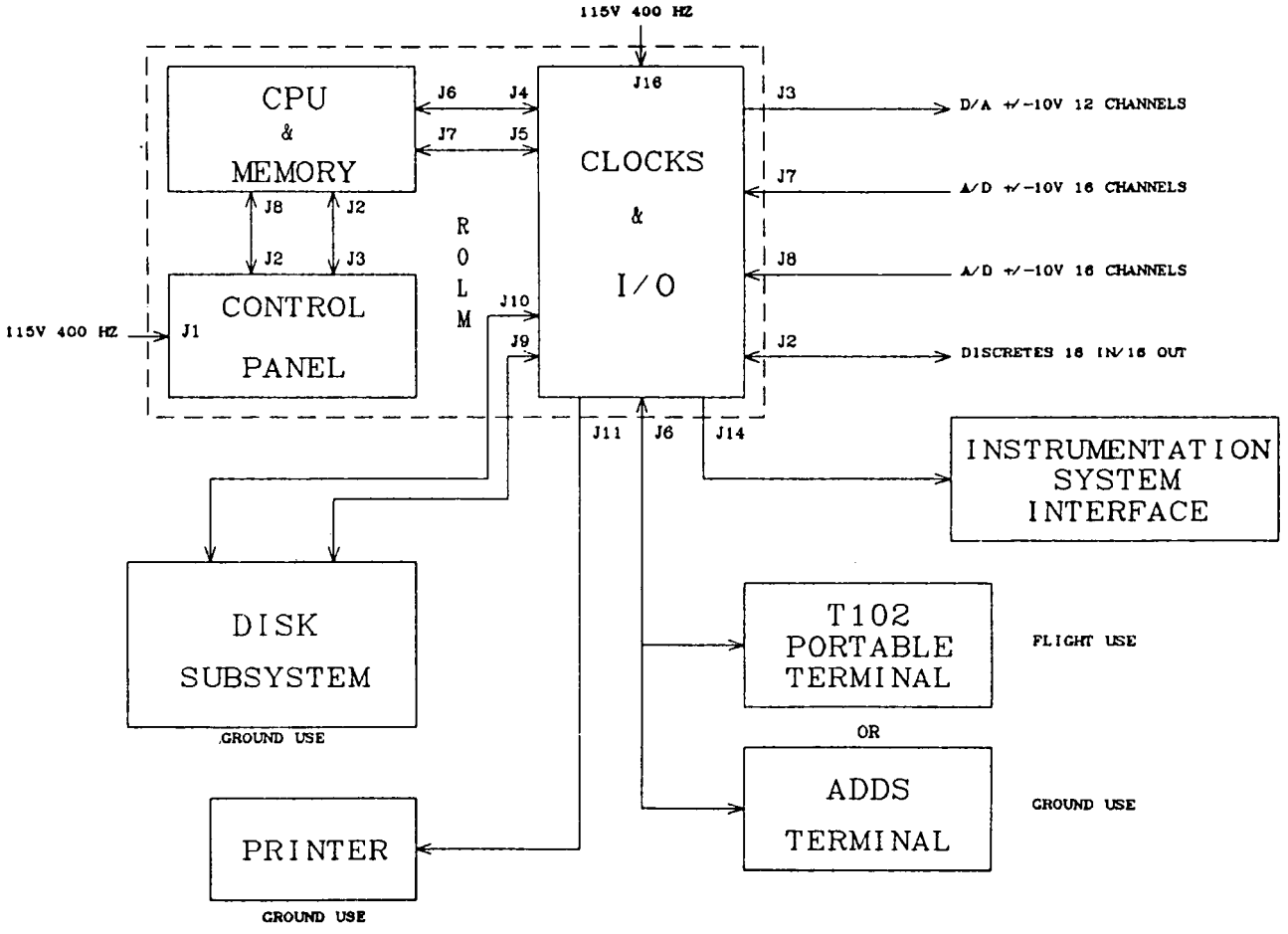

Figure 3.11 Rolm Computer System (NASA LaRC)

3.3.2. Sensor Package

The airplane states and controls are continuously measured by the sensor package. The set of sensors for the RQAS system is completely independent from any other sensors that may be used in the aircraft. It measures all states necessary for the RQAS operation. Table 3.2 gives a list of the required sensors and their accuracy. The α and β sensors are for documentation only. The angle of attack and sideslip sensors are installed on a noseboom. Since the measurement of α and β is impractical in a

Table 3.2 Sensor Requirements

Symbol	Sensor	Resolution	Range
A_x	Longitudinal Acceleration	0.0020 g	±1.0 g
A_y	Lateral Acceleration	0.0020 g	±0.5 g
A_z	Normal Acceleration	0.0024 g	-3 to +1 g
θ	Pitch Angle	0.5°	±30°
ϕ	Roll Angle	0.5°	±45°
p	Pitch Rate	0.5°/sec	±50°/sec
q	Roll Rate	0.5°/sec	±50°/sec
r	Yaw Rate	0.5°/sec	±50°/sec
δ_E	Elevator	0.5°	-15° to +25°
δ_A	Aileron	0.5°	±20°
δ_R	Rudder	0.5°	±32°
δ_{F1}	Right Outboard Flap	0.5°	±20°
δ_{F2}	Left Outboard Flap	0.5°	±20°
δ_{F3}	Inboard Flap	0.5°	±20°
α^1	Angle of attack	0.5°	-10° to +20°
β^1	Angle of Sideslip	0.5°	±20°
T	Static Temperature	2°F	-65° to +120°F
P_S	Static Pressure	0.010 psia (25 ft)	0 to 25k ft
P_D	Dynamic Pressure	0.005 psi (4 knots)	40 to 150 knots

[1] For documentation only

production system, the computer will estimate those angles for use in the control laws. The sensor package is installed on one of the pallets of the RQIS. Signal conditioners are provided to eliminate high frequency noise, e.g. engine vibrations, and to adapt the voltage range of the sensors to the A/D range of ±10V.

3.3.3 Data Recording System

All airplane states and some computed variables are recorded on a digital tape recorder, which is installed in the luggage compartment in the nose of the aircraft. The system, designed and fabricated by NASA LaRC, records 32 analog channels plus a number of digital channels on a PCM encoded stream tape. Figure 3.12 shows a list of the 32 analog channels that are recorded. Also given are the types of sensors to be used and the cutoff frequency for the anti-aliasing filters. These filters are necessary to avoid the phenomenon of aliasing. Aliasing occurs when a signal is sampled which has a frequency component higher than half the sampling frequency, i.e. the Nyquist frequency. The data are recorded in frames containing the actual data, time codes and monitor words. The format of each data frame is shown in Figure 3.13.

After each test flight the data are transferred to a micro computer with a cartridge hard disk. This allows storage of the flight data in a convenient way. The data can then be analyzed using either software on the micro computer, or, after transfer on a larger mainframe computer.

MEASUREMENT LIST

#	MEASUREMENT	SENSOR	RANGE	FILTER		STATUS		
				FLAT	CUTOFF	SENSOR	S/C	FILTER
1	LONGITUDINAL ACCELERATION	KISTER 303T	±1G	6	10	O		
2	LATERAL ACCELERATION	KISTER 303T	±0.5G	6	10	O		
3	NORMAL ACCELERATION	KISTER 303T	-3 TO +1G	6	10	O		
4	PITCH ATTITUDE	AVIONICS KVG 350	±30 DEG	6	10	L		
5	ROLL ATTITUDE	AVIONICS KVG 350	±45 DEG	6	10	L		
6	ROLL RATE	AVIONICS KRG 331	±50 DEG/SEC	6	10	L		
7	PITCH RATE	AVIONICS KRG 331	±50 DEG/SEC	6	10	L		
8	YAW RATE	AVIONICS KRG 331	±50 DEG/SEC	6	10	L		
9	ELEVATOR SURFACE	CPT	15 DOWN TO 25 UP	6	10	O		
10	RIGHT AILERON SURFACE	CPT	±20 DEG	6	10	O		

O - ON HAND L - LOAN P - PROCURE D - DESIGN

Figure 3.12 Measurement List (NASA LaRC)

MEASUREMENT LIST

#	MEASUREMENT	SENSOR	RANGE	FILTER		STATUS		
				FLAT	CUTOFF	SENSOR	S/C	FILTER
11	RUDDER SURFACE	CPT	±32 DEG	6	10			
12	RIDE OUT BOARD FLAP	CPT	±15 DEG	6	10			
13	LEFT OUT BOARD FLAP	CPT	±15 DEG	6	10			
14	LEFT IN BOARD FLAP	CPT	±15 DEG	6	10			
15	RIGHT IN BOARD FLAP	CPT	±15 DEG	6	10			
16	SEPARATE ELEVATOR SURFACE	CPT	±10 DEG	6	10			
17	ANGLE OF ATTACK	NASA VANE	-10° TO +20°	6	10			
18	ANGLE OF SIDESLIP	NASA VANE	±20 DEG	6	10			
19	TEMPERATURE	ROSEMOUNT 102-E	-65° TO 120° F	6	10			
20	STATIC PRESSURE	ROSEMOUNT	0 TO 25K FT	6	10			

O - ON HAND L - LOAN P - PROCURE D - DESIGN

Figure 3.12 (cont.) Measurement List (NASA LaRC)

MEASUREMENT LIST

#	MEASUREMENT	SENSOR	RANGE	FILTER		STATUS		
				FLAT	CUTOFF	SENSOR	S/C	FILTER
21	DYNAMIC PRESSURE	CELESCO	0 TO 230K KNOTS	6	10			
22	PILOT'S LONGIT. CONTROL POSITION	CPT	±5 INCHES	6	10			
23	PILOT'S LATERAL CONTROL POSITION	CPT	±100 DEG	6	10			
24	PILOT'S LONGIT. CONTROL FORCE	FORCE WHEEL	±75 LBS	6	10			
25	PILOT'S LATERAL CONTROL FORCE	FORCE WHEEL	±50 LBS	6	10			
26	LEFT AILERON SURFACE	CPT	±20° DEG	6	10			
27	INPUT VOLTAGE	(RIGHT OUT-BOARD FLAP)	TBD	6	10			
28	INPUT VOLTAGE	(LEFT OUT-BOARD FLAP)	TBD	6	10			
29	INPUT VOLTAGE	(RIGHT IN-BOARD FLAP)	TBD	6	10			
30	INPUT VOLTAGE	(LEFT IN-BOARD FLAP)	TBD	6	10			
31	INPUT VOLTAGE	SEPARATE ELEVATOR ACTUATOR	TBD	6	10			
32	INPUT VOLTAGE	RUDDER ACTUATOR	TBD	6	10			

Figure 3.12 (cont.) Measurement List (NASA LaRC)

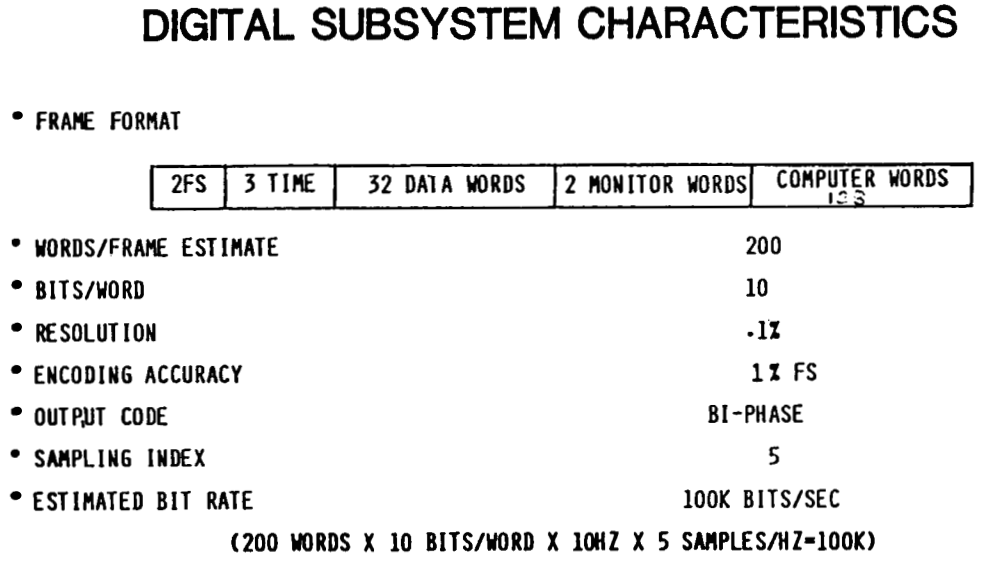

Figure 3.13 Data Frame Format (NASA LaRC)

3.3.4. Test Engineer's Panel

The test engineer's panel is the main control panel of the RQAS system. Its layout is shown in Figure 3.14. A set of gauges displays the actual and commanded position of all RQAS control surfaces, so that the test engineer can monitor the system activity in real time. In addition, indicator lights show the status of the locking actuators and limit switches. Switches for Rolm power, hydraulics, actuator signal engage, and a system disengage button are provided. The flight computer itself is controlled via the handheld terminal, which can be placed at either the pilot or test engineer's station. Separate controls for the Data Acquisition System (DAS) allow the

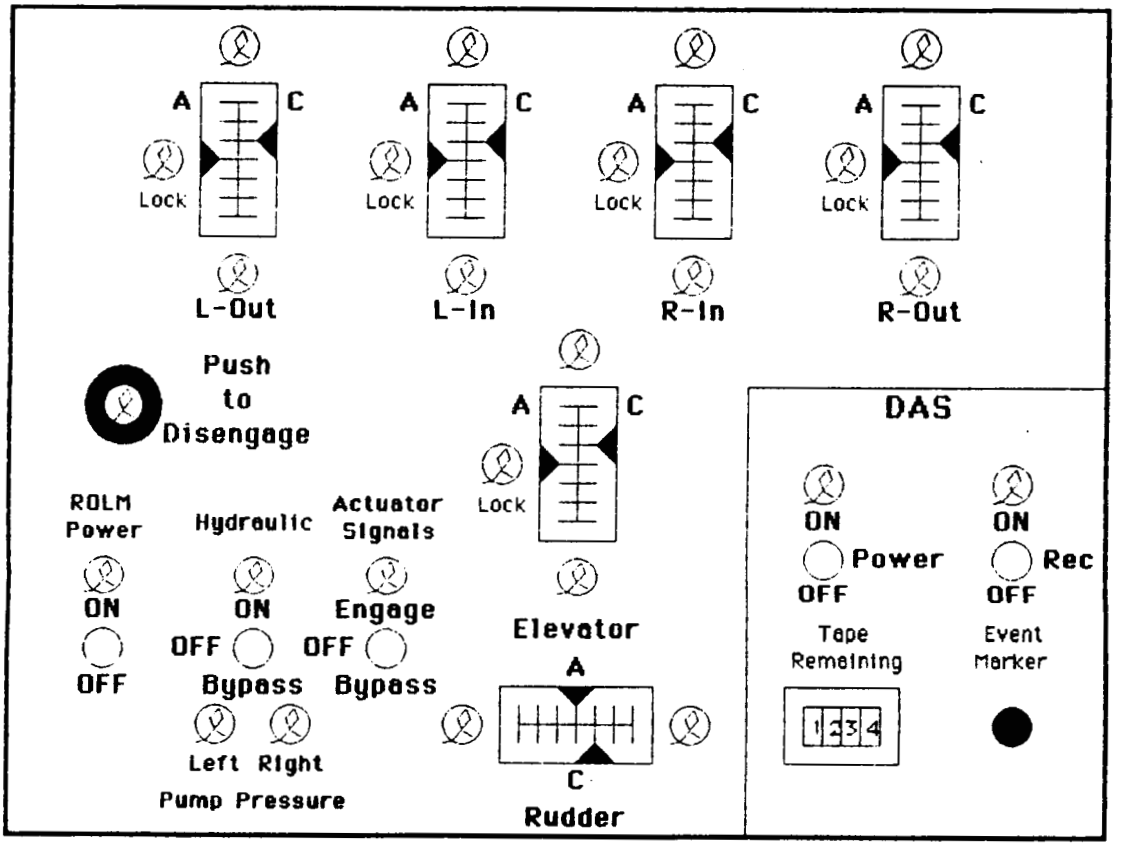

Figure 3.14 Test Engineer's Panel

test engineer to start and stop the data tape, mark the beginning of an experiment on tape, and see how much tape is remaining.

3.3.5. Pilot's Panel

The pilot control panel layout is shown in Figure 3.15. It allows the pilot to operate the RQAS system for demonstration flights. In this case the extended monitoring capabilities offered by the test engineer's panel are not required, and the pilot's panel therefore contains only a minimum number of switches. Included are the

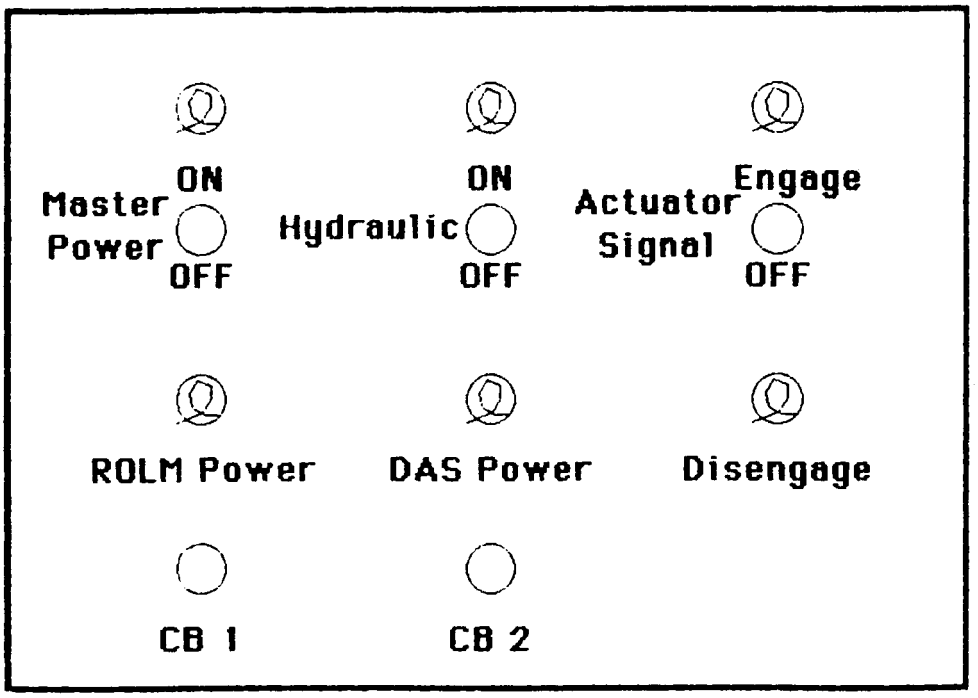

Figure 3.15 Pilot's Control Panel

master power switch for the entire system, a switch for the hydraulic, and the actuator signal engage switch. Indicator lights for Rolm power, DAS power and disengage are also provided. The pilot's disengage switch is installed on the yoke.

3.4. Overall Wiring Diagram

This Section discusses the RQAS wiring diagram which is shown in Figure 3.16. This diagram shows the connections between the main components of the RQAS. The sensor package and the data recording system are not shown. A parts list for the diagram is found in Appendix C. The diagram also defines the interface between hardware installed by NASA and hardware installed by Cessna. This interface

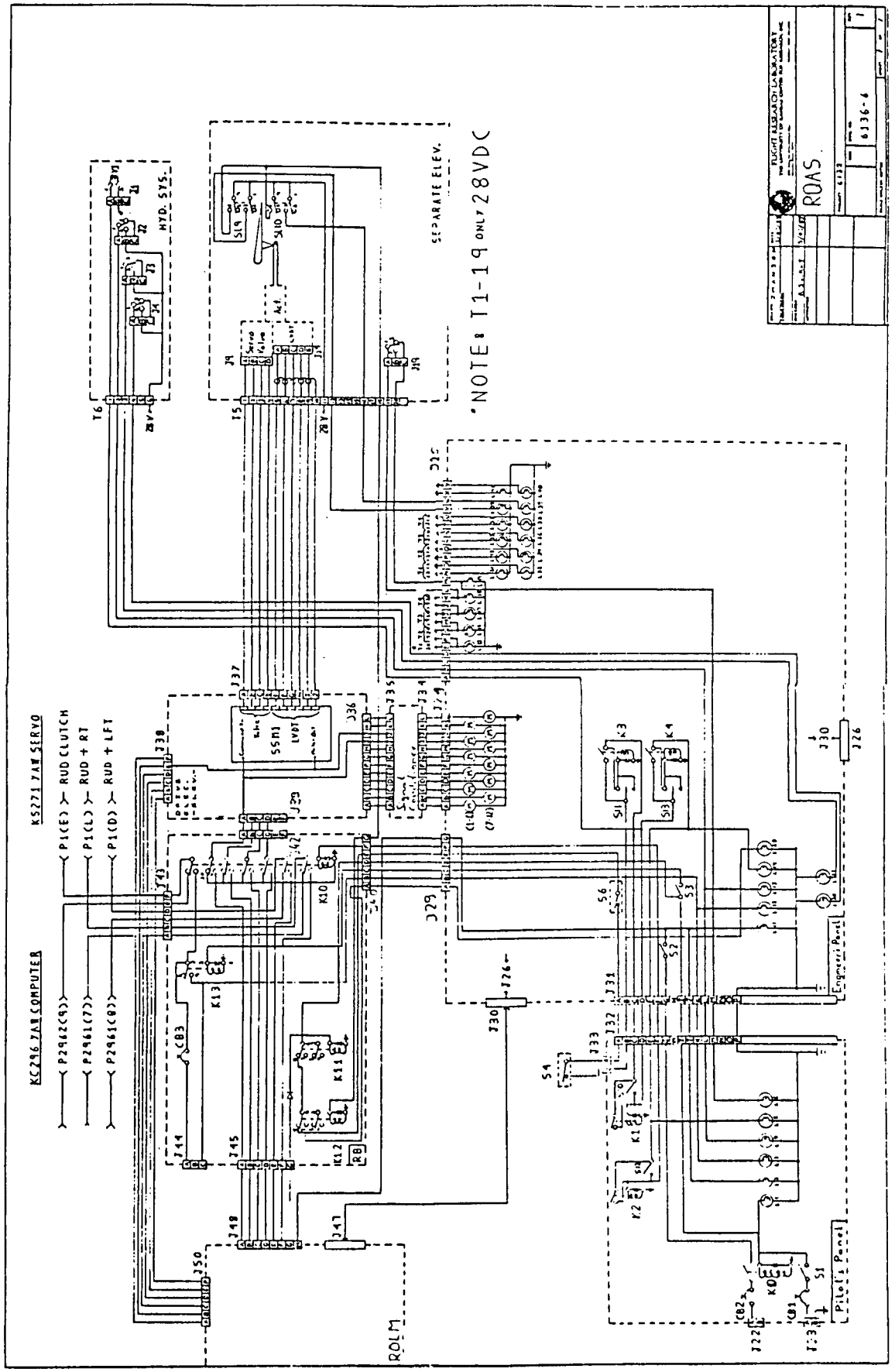

Figure 3.16 RQAS Wiring Diagram

ORIGINAL PAGE IS
OF POOR QUALITY

consists of a set of terminal strips, T1 - T6, where T1 - T5 contain the electrical connections to each of the separate RQAS control surfaces and T6 is the electrical connection to the hydraulic system. The RQAS is connected to the airplane power bus via J22 and J23.

Power is switched to the system with the pilot master power switch, S1. Then the test engineer closes his ROLM and DAS power switches, S2 and S3. Alternatively, for demonstration flights, the pilot can close S2 and S3 before take-off and activate the system in flight using only the master power switch. The 115 VAC needed by the ROLM and the DAS are switched with relays, K0 and K13. Indicator lights on both control panels show the system status. The hydraulic and signal engage switches, along with the disengage relays, are all connected in series, so that opening any one of them will fully disengage the system. The switches, S10 to S13, are 'push to activate' switches which will close a relay. The relays, K1 to K4, are wired such that they remain closed until their power is disconnected by an automatic or manual disengage. To activate the system, these switches need to be closed in the right sequence, since each switch enables the next in the series. The sequence is:

S11 Engineer panel hydraulic enable

S10 Pilot panel hydraulic activate

S13 Engineer panel signal enable

S12 Pilot panel signal engage.

For pilot only operation the switches on the engineer panel, S11 and S13, are closed before take-off, so that the pilot can operate the system using only the pilot panel and the handheld terminal.

Activating the hydraulic opens the shuttle valve. This applies hydraulic pressure to the actuators and to the locking actuators, which will then unlock. Also a

zero signal is send to the drive electronics, so that the control surfaces remain centered. When the signal engage switches are closed, relay K10 is activated and the computer signals are switched through to the drive electronics. At this point the RQAS is in operation. Any disengage will deactivate both K10 and the hydraulics, thereby sending a zero signal to the actuators, so the control surfaces can be centered with the pressure remaining in the accumulator and then be locked. The operating procedures are discussed in detail in Section 5.

3.5 Flight Software

The software developed for the RQAS system consists of the actual control algorithms and several data checking routines to increase system safety. The flight algorithms contain the trim map, the control law, estimators for α and β, and a maneuvering algorithm. A functional block diagram of the flight algorithms is given in Figure 3.17. The trim map computes trim values of the airplane states for the current dynamic pressure and elevator deflection. Both scheduling parameters are passed through a low pass filter to eliminate turbulence influences on the trim map computation. The trim data are then used to extract the state variable perturbations from the measurements obtained from the sensors. Estimators are used to infer the angle of attack and the angle of sideslip from the other states. The maneuvering algorithm separates turbulence induced perturbations from pilot induced maneuvering by comparing the actual airplane state at each sample point with a state computed from a linear model fed with the previous state and the pilot controls. This allows the control law to counteract just the turbulence and ignore pilot maneuvers. This is an important contribution to the airplane handling qualities, because otherwise the

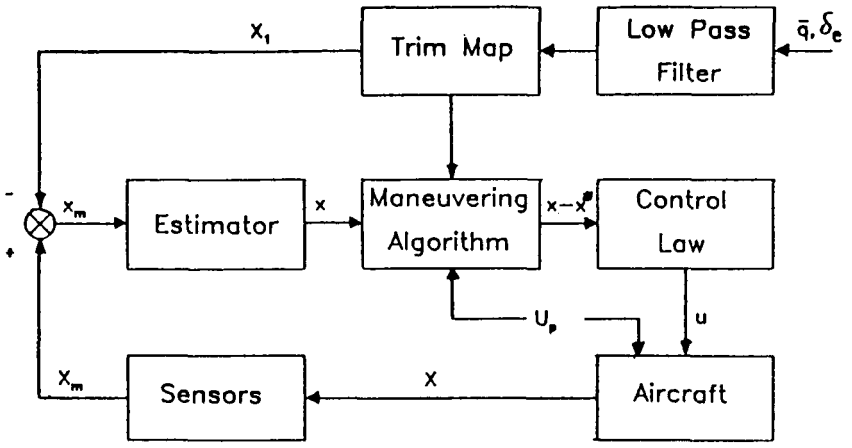

X airplane states

X_m measured states

X_1 airplane trim states

x_m perturbations from trim in measured states

x perturbations from trim in states used in control law

$x - x^*$ deviation from desired state

U_p pilot commands

u RQAS control commands

Figure 3.17 RQAS Flight Algorithm

controller, being a closed loop feedback controller, would try to maintain the current trim state and fight any maneuver the pilot might attempt.

3.5.1. Control Laws

As it was mentioned in section 2.4, the control laws are based on two different optimal control formulations. The fundamental approach in optimal control is to find a control history **u** that minimizes a quadratic cost function. The system is given in state

space form (Eqn. (2.4)) and the cost functions for output weighting and for control rate weighting are stated in Eqns. (2.5) and (2.6). The continuous problem can be shown to be equivalent to a discrete problem (Reference 8), that has as its system equation,

$$\mathbf{x}_{k+1} = \Phi\mathbf{x}_k + \Gamma\mathbf{u}_k \tag{3.1}$$

where

$$\Phi = e^{\mathbf{A}T} \quad , \quad \Gamma = \int_0^{\infty} \{ (e^{\mathbf{A}T}) dt \} \ \mathbf{B} \ dt \tag{3.2}$$

The output of the system is given by

$$\mathbf{y}_k = \mathbf{C}\mathbf{x}_k + \mathbf{D}\mathbf{u}_k \tag{3.3}$$

The solution to this problem has been derived by Dorato (Reference 9). It is the linear full state feedback control.

$$\mathbf{u}_k = -\mathbf{K}\mathbf{x}_k \tag{3.4}$$

Computer programs exist to compute the gain matrix **K** from the input matrices **A**, **B**, **C**, **D**, the weighting matrices **Q** and **R**, and the sample time T (References 10 and 11). The performance of any set of gains is judged from simulation results. The weighting matrices are changed by the designer, until a satisfactory design is achieved. The gain matrices for all flight conditions are listed in Appendix B.

3.5.2 Estimators

Since measuring the angle of attack and the angle of sideslip is impractical for a production system, the RQAS system employs an estimation algorithm to infer α and β from the other states. The performance of the estimators will be evaluated using the data recorded during test flights, where both the measured and the estimated values of α and β can be recorded on tape.

Estimates of α and β will be computed as a linear combination of states and controls, where the state vector is augmented by the accelerations. Thus the estimators can be formulated by applying gains to the output vector:

$$\hat{\alpha} = - [K_{\alpha_1} \quad K_{\alpha_2} \quad K_{\alpha_3} \quad K_{\alpha_4}] [a_z \quad u \quad q \quad \theta]' - [K_{\alpha_5} \quad K_{\alpha_6} \quad K_{\alpha_7}] [\delta_{se} \quad \delta_f \quad \delta_e]' \tag{3.5}$$

$$\hat{\beta} = - [K_{\beta_1} \quad K_{\beta_2} \quad K_{\beta_3} \quad K_{\beta_4}] [a_y \quad p \quad r \quad \phi]' - [K_{\beta_5} \quad K_{\beta_6} \quad K_{\beta_7}] [\delta_r \quad \delta_{df} \quad \delta_a]' \tag{3.6}$$

To obtain the gains for the α estimator, consider the lift equation for small perturbations from steady-state flight given in body-axes (Reference 7):

$$m(\dot{w} - U_{B1}q) = - mg\theta\sin\theta_1 + f_z \tag{3.7}$$

Dividing by m and realizing that

$$\dot{w} \approx U_1\dot{\alpha} \quad \text{and} \quad U_B = U_1\cos\alpha_1$$

Equation (3.7) becomes

$$a_z = U_1\dot{\alpha} - U_1\cos\alpha_1 q + g\sin\theta_1\theta \tag{3.8}$$

From the linear model it follows that

$$\dot{\alpha} = A_{11}\alpha + A_{12}u + A_{13}q + A_{14}\theta + B_{11}\delta_{se} + B_{12}\delta_f + B_{13}\delta_e \tag{3.9}$$

where A_{ij} and B_{ij} are elements of the longitudinal system dynamics and control effectiveness matrices. Substituting Eqn (3.9) into Eqn (3.8) and solving for α yields:

$$\hat{\alpha} = -\begin{bmatrix} \frac{-1}{U_1 A_{11}} & \frac{A_{12}}{A_{11}} & \frac{A_{13}-\cos\alpha_1}{A_{11}} & \frac{A_{14}+(1/U_1)g\sin\theta_1}{A_{11}} \end{bmatrix} \begin{bmatrix} a_z \\ u \\ q \\ \theta \end{bmatrix} - \begin{bmatrix} \frac{B_{11}}{A_{11}} & \frac{B_{12}}{A_{11}} & \frac{B_{13}}{A_{11}} \end{bmatrix} \begin{bmatrix} \delta_{se} \\ \delta_f \\ \delta_e \end{bmatrix} \tag{3.10}$$

In a similar way the sideslip estimator is computed:

$$\hat{\beta} = -\begin{bmatrix} \frac{-1}{U_1 A_{11}} & \frac{A_{12}-\sin\alpha_1}{A_{11}} & \frac{A_{13}+\cos\alpha_1}{A_{11}} & 0 \end{bmatrix} \begin{bmatrix} a_y \\ p \\ r \\ \phi \end{bmatrix} - \begin{bmatrix} \frac{B_{11}}{A_{11}} & \frac{B_{12}}{A_{11}} & \frac{B_{13}}{A_{11}} \end{bmatrix} \begin{bmatrix} \delta_r \\ \delta_{df} \\ \delta_a \end{bmatrix} \tag{3.11}$$

where the A_{ij} and B_{ij} are now elements of the lateral matrices. The estimator gains are summarized in Table 3.3.

3.5.3 Maneuvering Algorithm

As mentioned, a pure regulator will attempt to cancel all accelerations, including those desired by the pilot. Therefore, it will oppose the pilot when he tries to maneuver the airplane, which would result in a drastic reduction in handling qualities. This can be avoided by using a maneuvering algorithm, or model following, which follows a command model, e.g. the unaugmented airplane with pilot inputs.
The airplane motion is given as

$$\mathbf{x}_{k+1} = \Phi\mathbf{x}_k + \Gamma\mathbf{u}_k + \Gamma_p\mathbf{u}_{pk} \tag{3.12}$$

where $\mathbf{u}$ are the RQAS controls

$\mathbf{u}_p$ are the pilot controls.

A command model can also be generated:

$$\mathbf{x}_{mk+1} = \Phi_m\mathbf{x}_k + \Gamma_p\mathbf{u}_{pk} \tag{3.13}$$

Using as the controller implementation

$$\mathbf{u}_k = -\mathbf{K}(\mathbf{x}_k - \mathbf{x}_{mk}) \tag{3.14}$$

the regulator will try to drive the difference between the model states and the actual airplane states to zero. Note that on the right hand side of Eqn (3.13) the actual airplane state is used instead of the model state. This prevents the controller from

Table 3.3 Estimator Gains

Gain	FC#1	FC#2	FC#3	FC#4	FC#5
K_{α_1}	0.0046	0.0036	0.0035	0.0023	0.0046
K_{α_2}	0.0015	0.0011	0.0009	0.0004	0.0016
K_{α_3}	0.0679	0.0580	0.0530	0.0328	0.0621
K_{α_4}	-0.0179	-0.0102	-0.0102	-0.0035	-0.0190
K_{α_5}	0.0307	0.0292	0.0291	0.0278	0.0272
K_{α_6}	0.2120	0.2141	0.2135	0.2140	0.2112
K_{α_7}	0.1537	0.1460	0.1456	0.1388	0.1361
K_{β_1}	0.0352	0.0252	0.0252	0.0152	0.0360
K_{β_2}	-0.0007	-0.0004	0.4523	-0.0001	-0.0007
K_{β_3}	0.0056	0.0049	0.0045	0.0026	0.0055
K_{β_4}	0.0000	0.0000	0.0000	0.0000	0.0000
K_{β_5}	0.0356	0.0337	0.0337	0.0316	0.0364
K_{β_6}	-0.2701	-0.2584	-0.2585	-0.2465	-0.2744
K_{β_7}	0.0356	0.0377	0.0337	0.0316	0.0364

integrating model errors, which would cause the control surfaces to move slowly to their limit position. By using the linearized airplane model in the command model equation, the augmented airplane will behave essentially like the unaugmented airplane and it will not counteract the pilot controls.

3.5.4 Safety Checks

Several safety checks incorporated into the software can trigger an automatic disengage of the system in case of any unreasonable input or output signal. Such signals can be caused by faulty sensors or errors in the computer program and a variety of other causes. The algorithm basically checks for signals that are out of range, i.e. outside a range defined as reasonable for each particular variable, signals that are frozen at any value for longer than a given time period, and signals that are wildly fluctuating, i.e. whose rate of change is larger than what is defined to be reasonable. If any of these conditions occurs for any of the sensed input or output variables, the computer will disengage the entire RQAS system, and an error flag is set. This error flag can be read by the test engineer using the handheld terminal and it will also be written on the tape, thus allowing the test engineer to determine the exact cause of the disengage.

3.5.5 System Checkout Software

Two computer programs will be provided to check both the system hardware and software. The sensor check program checks sensor signals during flight while the

ground check program checks the flight computer, A/D and D/A boards, the actuators, and the controller software.

3.5.5.1. Ground Check Program

This computer program provides the capability of a complete end to end check of the RQAS hardware and software with the exception of the sensor package. The program runs on the ground based micro-computer as part of the preflight check procedure. The ground computer needs to be interfaced to the RQAS in such a way, that it can send simulated sensor signals to the flight computer and read the flight computer control commands and the control surface positions. With the flight software running on the Rolm computer, precomputed sensor signals are send to the Rolm and the resulting control commands and/or control surface deflections are read and

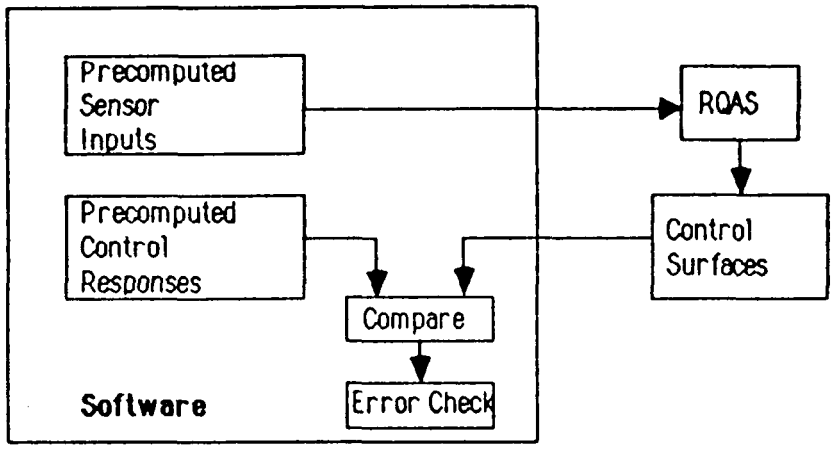

Figure 3.18 Ground Check Program

compared with precomputed values. If the difference exceeds the specified tolerance level, an error message is displayed on the screen of the ground computer. A block diagram of this program is shown in Figure 3.18.

The precomputed signals contain sensor signals that will exercise all automatic disengages provided in the RQAS software. Sensor signals can also be generated by exciting a math model of the airplane with a gust model and the control commands generated by the flight computer. Therefore all disengage paths as well as proper operation of the entire system can be tested with this program.

3.5.5.2. Sensor Check Program

This computer program verifies that the sensors are operating correctly prior to engaging the RQAS. It is executed on the Rolm computer during flight; however, the

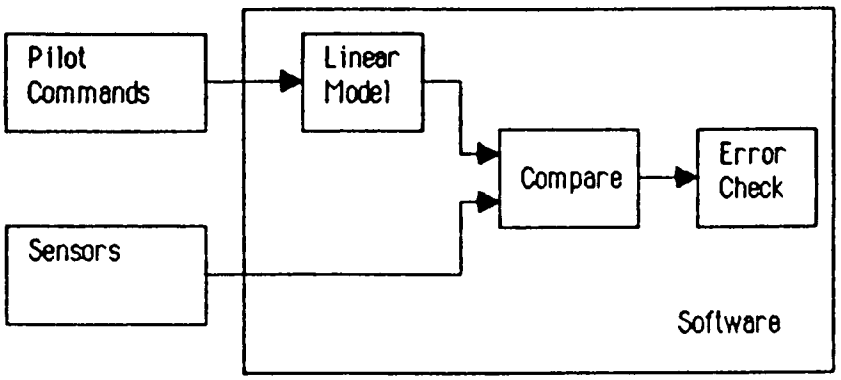

Figure 3.19 Sensor Check Program

hydraulic system is not on, so the RQAS surfaces stay locked during its execution. To execute the check, the airplane is flown at a specified flight condition, for which a linear model of the airplane is stored in the flight computer. The pilot then maneuvers about that trimpoint, and the computer program compares the airplane states measured by the sensors with airplane states computed from the linear model excited by the pilot commands. If the difference between the states exceeds a specified tolerance, an error flag is set indicating a faulty sensor. A block diagram of this program is given in Figure 3.19.

In the above section the various components of the software have been discussed in detail. These include the flight software, consisting of the control law, the estimators for angle of attack and sideslip, and the maneuvering algorithm, and the system checkout software, consisting of the ground check and the sensor check program.

4 Projected Performance

This chapter discusses the performance predictions for the RQAS system. These predictions are based on linear simulations and frequency domain analysis. The linear simulation results are given in Section 4.1 and power spectral densities in Section 4.2. Simulation results for the maneuvering algorithm are discussed in Section 4.3. The open loop and closed loop eigenvalues for the aircraft are given in Appendix D.

4.1 Linear Simulation Results

For these simulations the linear model of the aircraft is excited by a Dryden gust model with a probability of exceedance of 10^{-3}, which corresponds to moderate turbulance. The Dryden spectrum is a commonly used representation of atmospheric turbulence and is given by (Reference 12):

$$\Phi_{\alpha g}(\omega) = \sigma_w^2 \frac{L_w}{\pi V_a^3} \frac{1 + 3(L_w\omega/V_a)^2}{[1 + (L_w\omega/V_a)^2]^2} \tag{4.1}$$

$$\Phi_{\beta g}(\omega) = \sigma_v^2 \frac{L_v}{\pi V_a^3} \frac{1 + 3(L_v\omega/V_a)^2}{[1 + (L_v\omega/V_a)^2]^2} \tag{4.2}$$

where, for clear-air turbulence,

σ_w is taken from Figure 2.1,

σ_v is found from the relationship

$$\frac{\sigma_w^2}{L_w} = \frac{\sigma_v^2}{L_v} \tag{4.3}$$

where

Above h = 1750 ft, $L_W = L_V = 1750$ ft

Below h = 1750 ft, $L_W = h$ ft

$$L_V = 145\ (h)^{1/3}\ \text{ft}$$

One way of measuring the performance of the RQAS is to calculate the rms value of the accelerations. This is a simple index which has a direct relation to the passenger comfort rating. It can be seen from Eqn (2.3) that the rms vertical acceleration, $\bar{a}_z$, has almost the same effect on comfort rating as lateral acceleration, $\bar{a}_y$. In flight, however, lateral acceleration is usually much smaller, because for most airplanes C_{Y_β} is smaller than C_{L_α}, and, as Eqns (2.1) and (2.2) show, the acceleration due to gust is directly proportional to C_{L_α} and C_{Y_β}, respectively.

The range of comfort rating for the closed-loop airplane is shown in Figure 4.1. Due to the fact that the lateral acceleration was neglected during the establishment of the design goal, the desired 80% passenger satisfaction (a comfort rating of 4) is not achieved over the entire envelope. There is, however, a large increase in passenger satisfaction over the flight envelope.

The actual rms predictions for the accelerations are given in Figure 4.2. These plots show the aircraft rms accelerations for five conditions, open loop, output weighting (OW), control rate weighting (CRW), and output weighting and control rate weighting with limited outboard flap travel. Since the RQAS does not require large flap deflections in flight conditions 3 and 4 (5,000 ft climb and 20,000 ft cruise), reducing the outboard flap travel to ±8 degrees for safety reasons has no adverse effect on the performance of the RQAS. However, for the other flight conditions, some

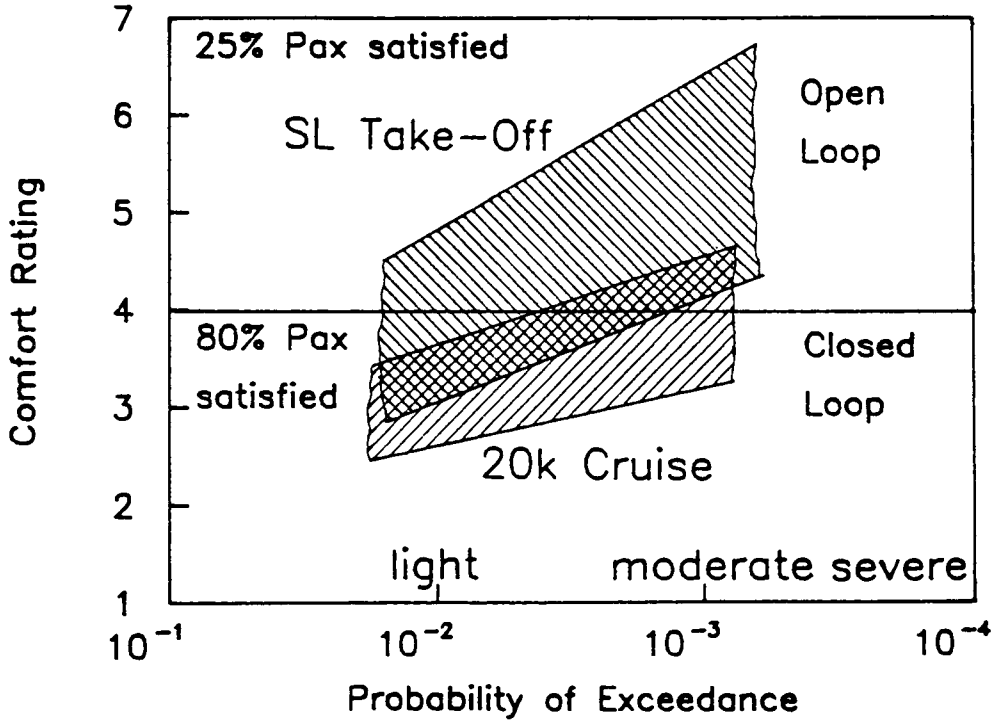

Figure 4.1 Closed-Loop Comfort Rating

reduction in performance occurs. Another observation is that the two controller algorithms perform almost equally well. It can be seen that the RQAS achieves a large reduction in both $\bar{a}_z$ and $\bar{a}_y$. The $\bar{a}_z$ reduction is between 40 and 50% of the open loop values using the full flap travel. Thus the design goal is easily met for all flight conditions. However, limiting the flap travel to ±8 degrees, which is required for safety reasons, slightly reduces the performance of the system in the take-off and approach flight conditions. The system will not be able to meet the design goal in this configuration. It can be observed from the figures that as the normal and lateralaccelerations are significantly reduced, the longitudinal accelerations are amplified

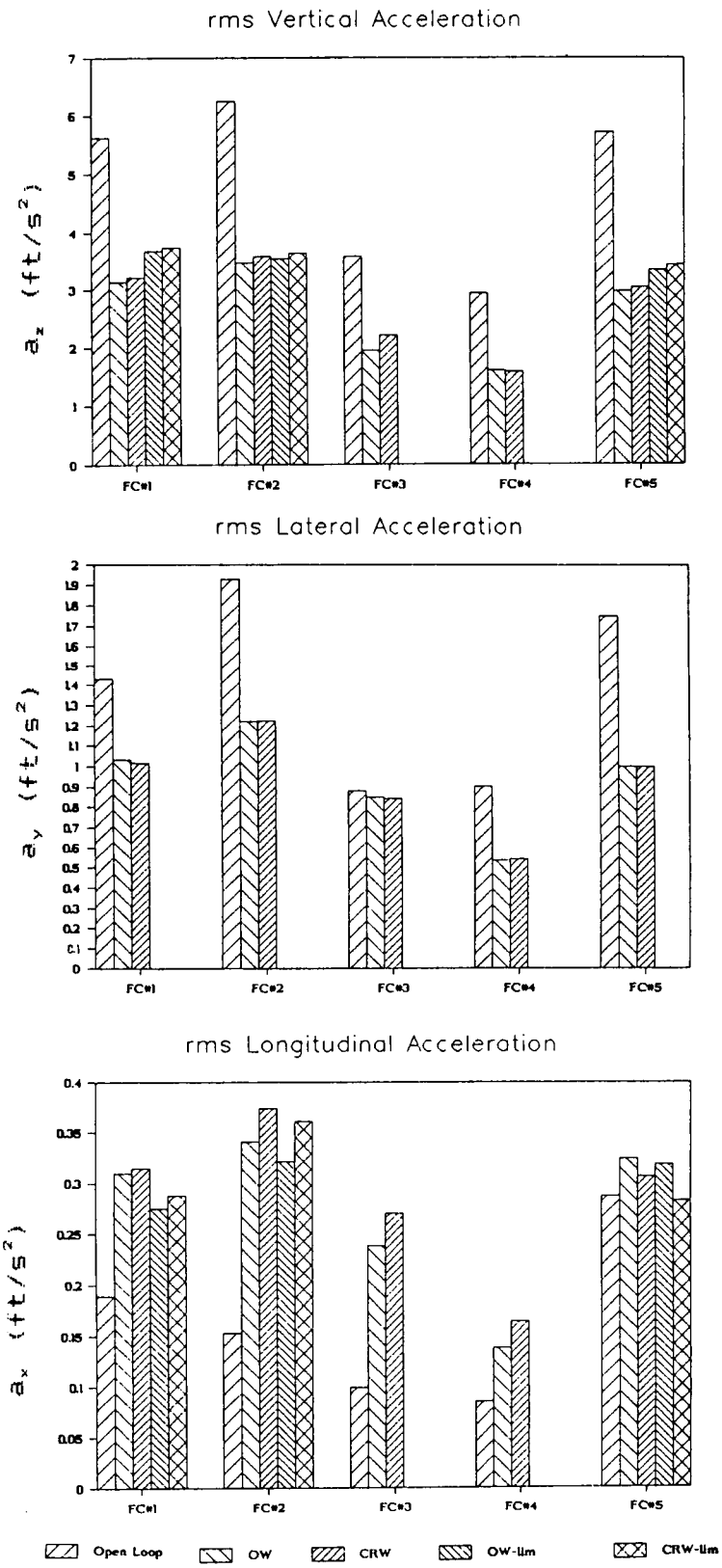

Figure 4.2 Performance Prediction: rms accelerations

by the system. Its magnitude remains quite small, and it is not expected to have an adverse effect on the perceived quality of the ride.

4.2 Frequency Domain Analysis

The evaluation of the controller designs in the frequency domain is done using power spectral density plots. These plots show a power spectrum of the airplane motion due to gust for both the unaugmented (open loop) and the augmented (closed loop) airplane in the five flight conditions. These plots are shown in Figure 4.3 to Figure 4.7. They demonstrate the same basic results for all five flight conditions. It can be seen that the main contribution to the reduction in $\bar{a}_z$ is in the frequency range from 0.1 - 3 rad/sec, at which people are most likely to get motion sickness. The percentage of passengers to get motion sickness is plotted over gust frequency in Figure 4.8. At higher frequencies, the open and closed loop curves approach each other due to the limited bandwidth of the RQAS. Note that the output weighting algorithm performs better at high frequencies than the control rate weighting algorithm. This should be expected since control rate weighting penalizes high control surface deflection rates and thereby limits the bandwidth of the controller. The a_x plots demonstrate the increase in longitudinal acceleration due to the controller. However, the value of $\bar{a}_x$ is still small enough to be of no concern. The a_y plots show that the controller increases lateral acceleration at low frequencies. The rms value of the acceleration is given by the square root of the integral of the PSD curve. Since the main contribution to the open loop rms value is the dutch roll peak, which is well damped in the closed loop case, the rms value is reduced significantly and passenger comfort is enhanced.

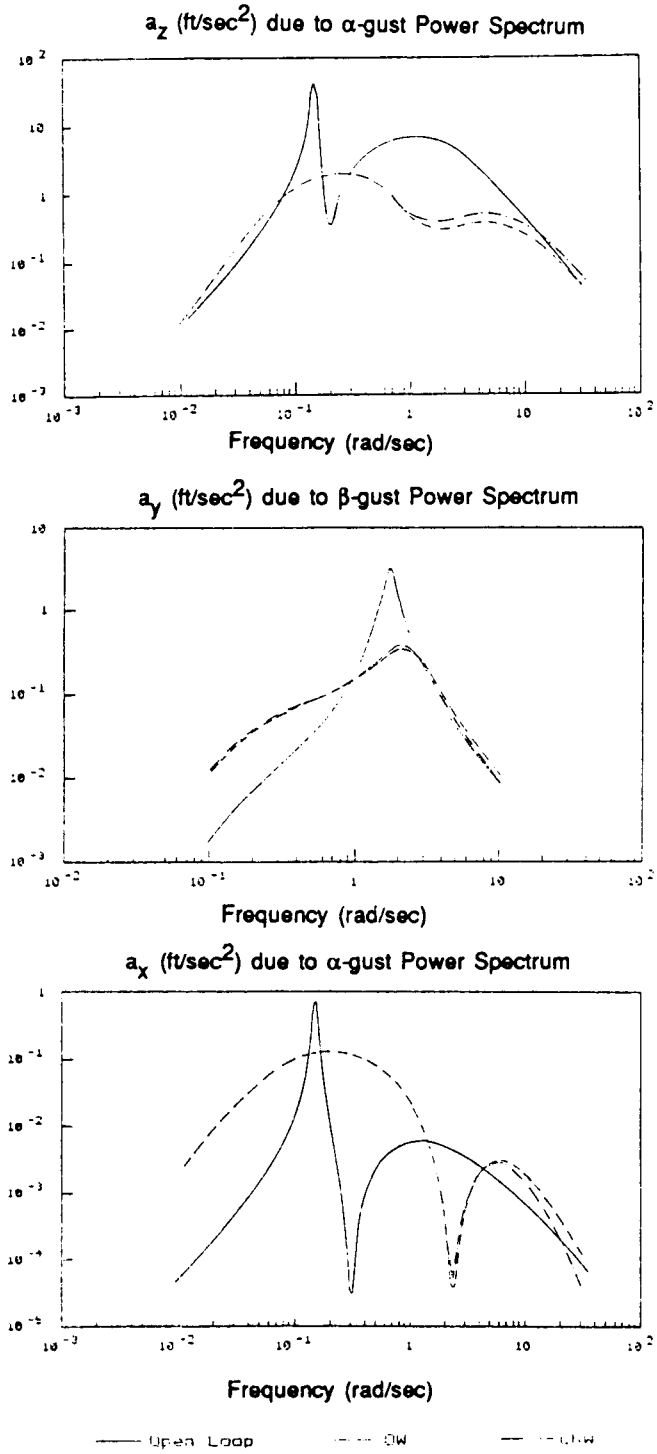

Figure 4.3 PSD Plots, Flight Cond. 1

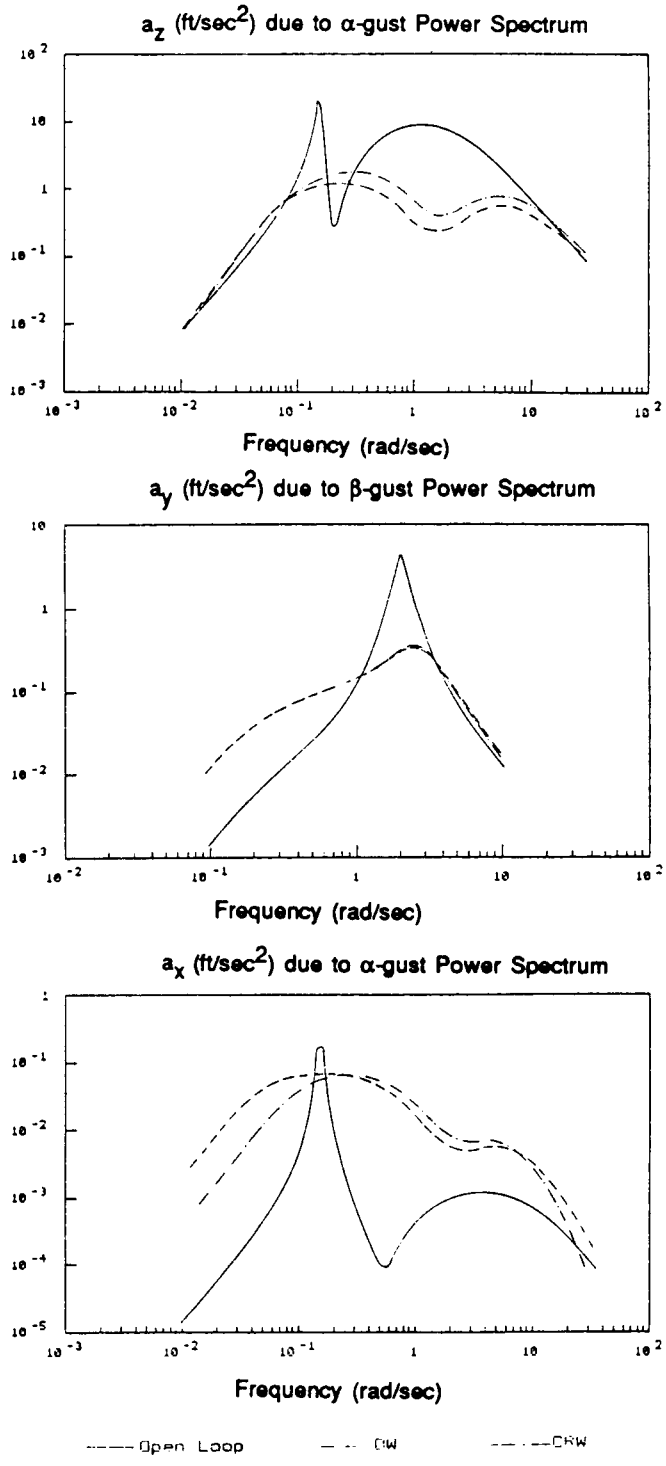

Figure 4.4 PSD Plots, Flight Cond. 2

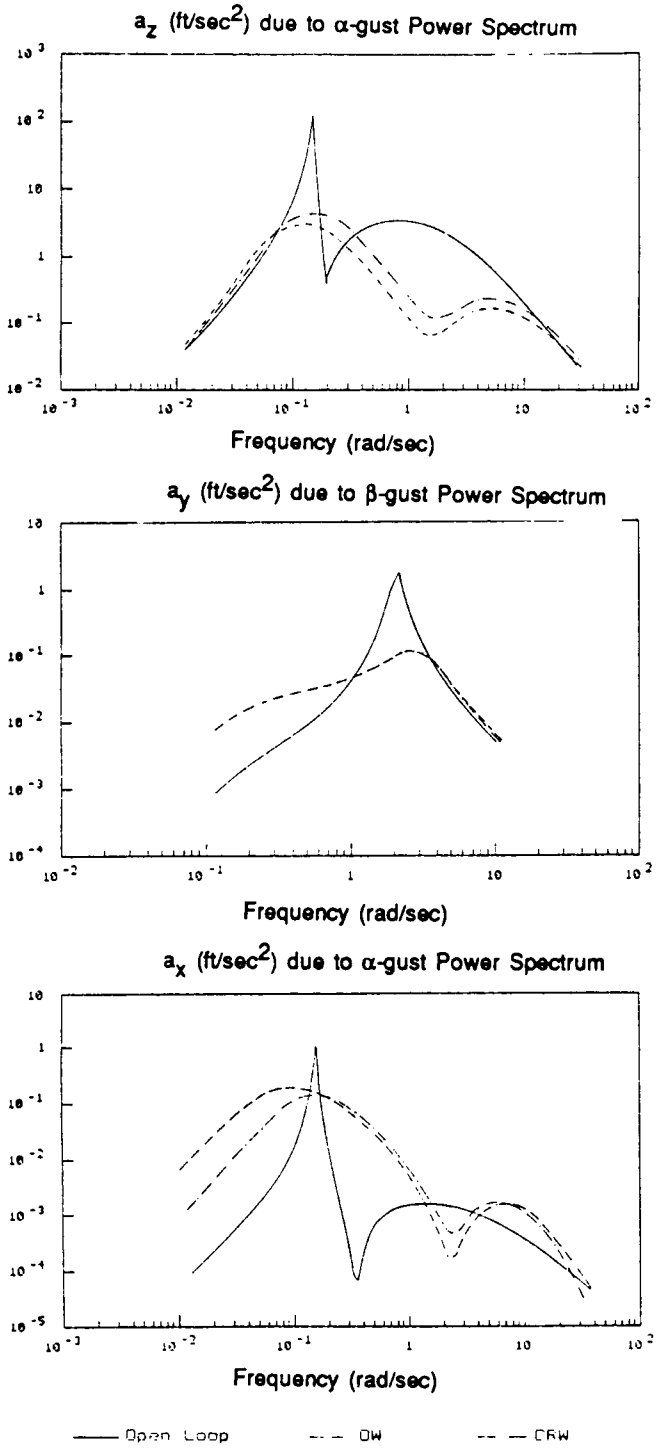

Figure 4.5 PSD Plots, Flight Cond. 3

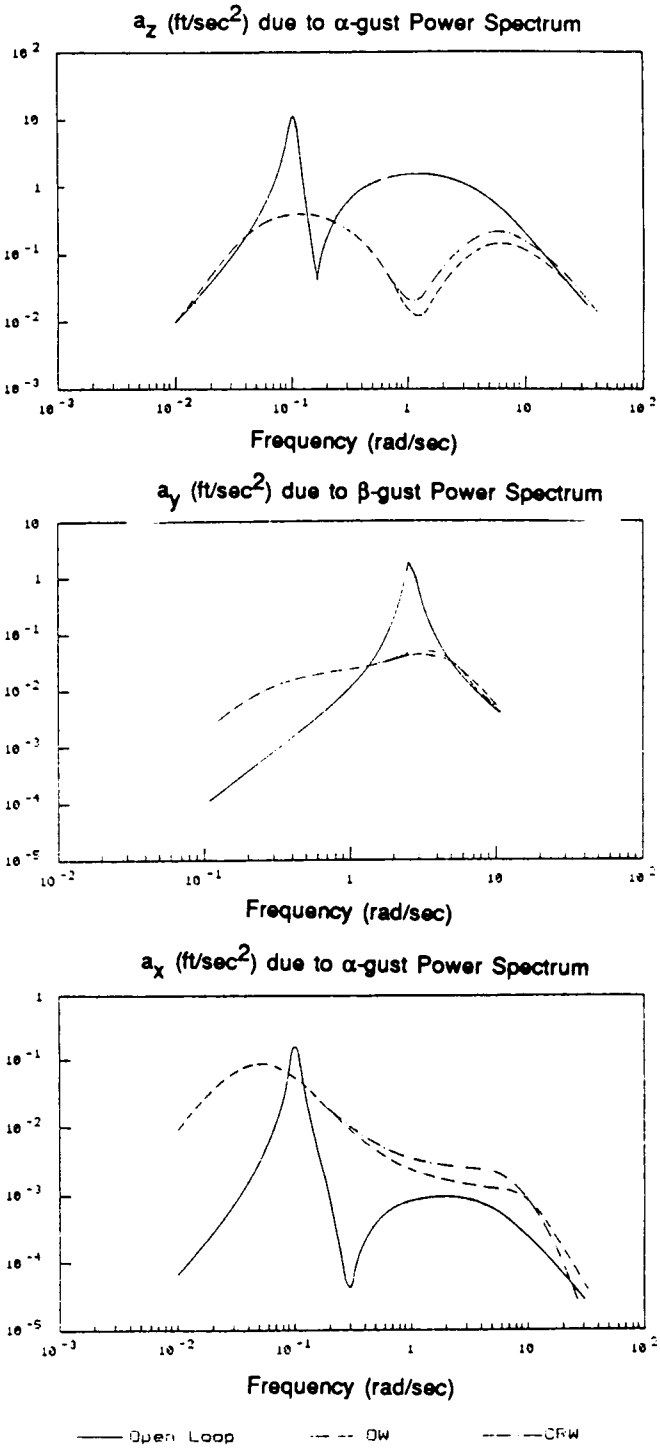

Figure 4.6 PSD Plots, Flight Cond. 4

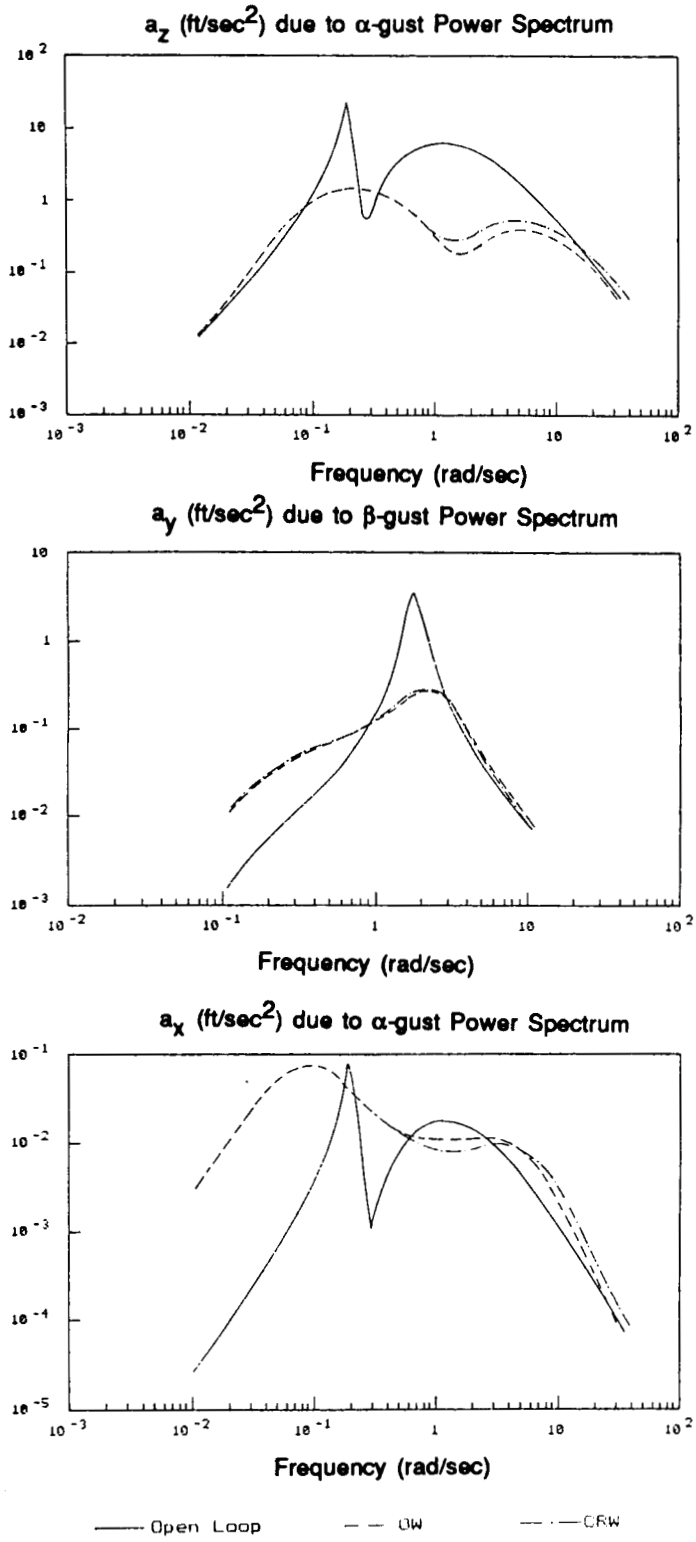

Figure 4.7 PSD Plots, Flight Condition 5

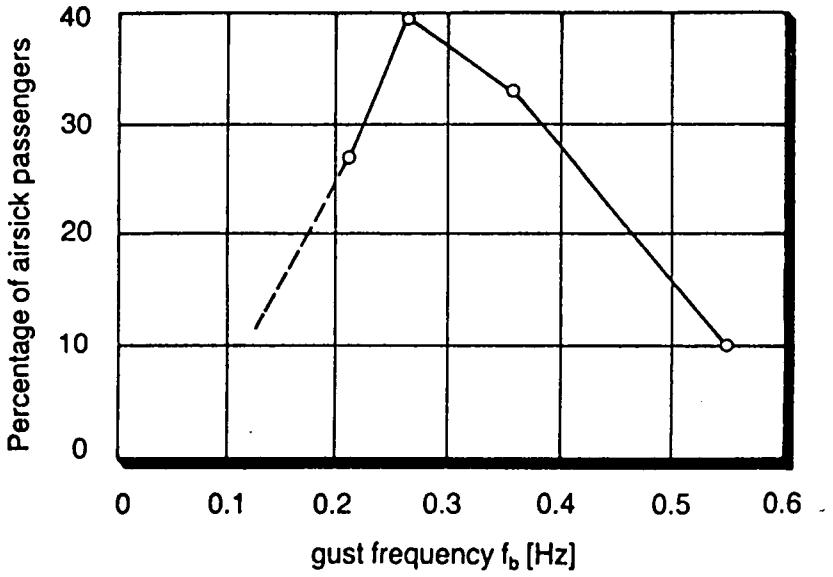

Figure 4.8 Motion Sickness Range (Reference 13)

The seemingly poor performance of the controller in cancelling low frequency lateral accelerations stems from the selection of the weighting matrix elements. The current design puts the main weights on sideslip and yaw rate rather than on the lateral acceleration so that the lateral controller mainly acts as a yaw damper.

Overall one can see that the two controller designs yield almost identical results. This can be explained by looking at the design procedure. For each controller designs weighting matrices have been selected that result in a controller with maximum performance that satisfies the design constraints of both control deflection limits and control rate limits. Therefore both controllers are subject to the same bandwidth limitations and performance goals and hence the results are nearly identical. Since the output weighting algorithm is simpler, it does not need to feedback control positions as the control rate weighting algorithm does, it is recommended as the primary design algorithm. However, both controller algorithms will be used in the research flights.

4.3 Maneuvering Algorithm Simulation

To demonstrate the effect of the maneuvering algorithm, which is a form of explicit model following, one sample case is presented here. The pilot input is a one second step input to the ailerons, a pause of four seconds, and a one second step in the opposite direction. The airplane should bank into a turn and after four seconds return to straight and level flight.

In Figure 4.9 the bank angle, sideslip, and differential flap deflection as from a linear simulation are plotted for three cases: open loop, RQAS on, RQAS + maneuvering algorithm on. It is clearly seen that the basic RQAS fights the pilot input. The moment the airplane starts to roll, the controller moves the differential flaps to counteract the motion. The maneuvering algorithm, on the other hand, completely ignores the motion, since the command model goes through the same maneuver. The curves for open loop and RQAS + maneuvering algorithm are identical, and the RQAS control surfaces do not move at all. The algorithm cannot, however, be expected to work this accurately in the actual airplane. It is only exact, when the command model exactly describes the airplane dynamics. This is the case in the linear simulation presented here.

The sideslip shows the excitation of the dutch roll mode in this maneuver. As the RQAS has a high damping on all oscillatory modes, the dutch roll oscillation is much reduced with the basic RQAS on. The use of the command model, however, reintroduces the low damping of the unaugmented airplane. The RQAS requires all the rudder, the pilot can therefore not fully coordinate his turns. A command model could be generated, that will automatically perform this task. In addition, a command model could be generated which has better dynamic characteristics, i.e. higher dutch

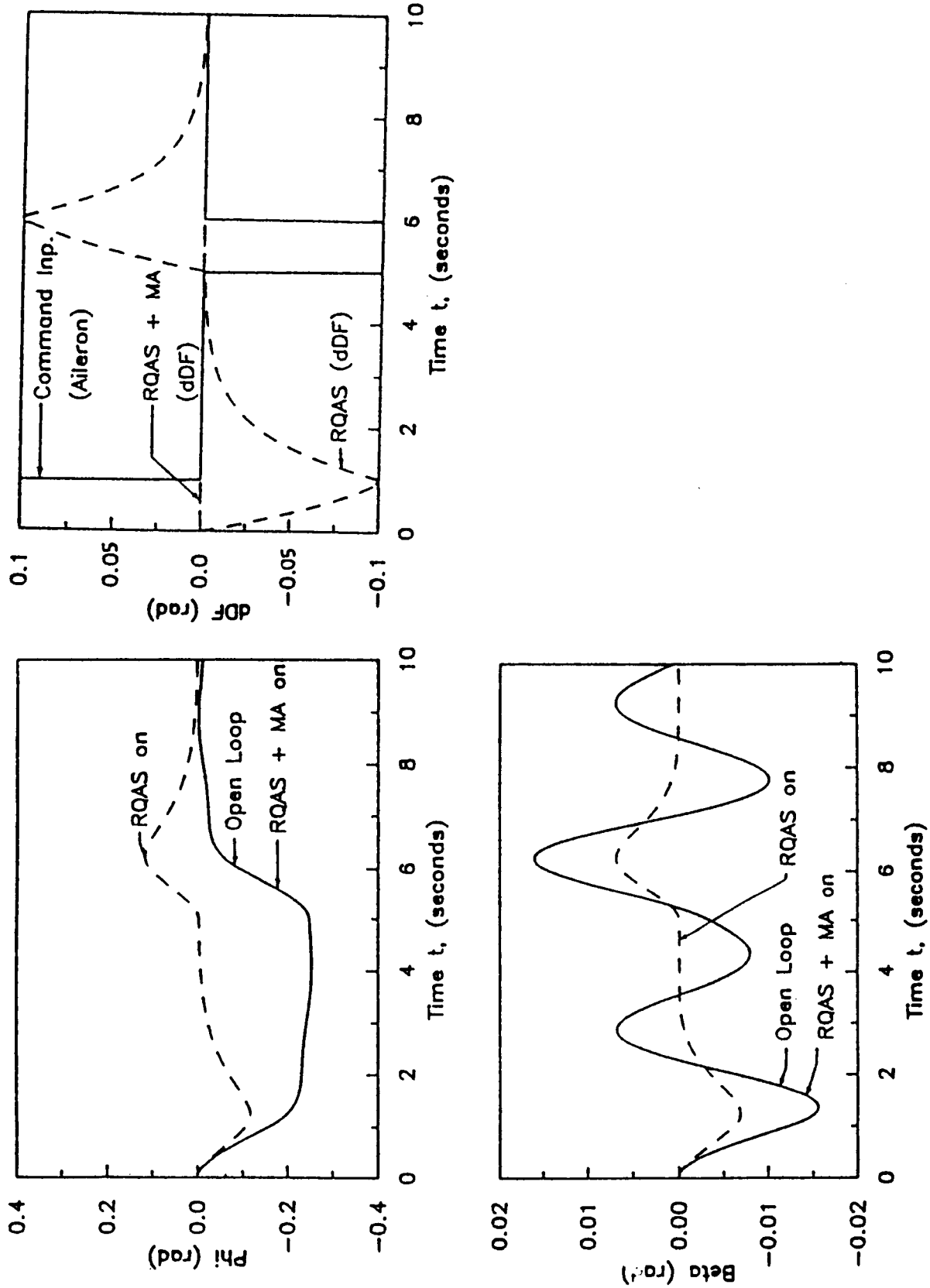

Figure 4.9 Maneuvering Simulation

roll damping, than the open loop airplane. This could be used to improve the handling qualities of the airplane.

5 Proposed System Operation

This chapter discusses the operational procedures to be used in the research flight program. These include the basic system operating procedures, system checkout procedures, and general procedures for the test flights. The basic system operating procedures (Section 5.1) contain two parts: First the system operation in normal test flights, second the emergency procedures. A detailed description of the function of each switch on the engineer's and pilot's control panels and a check-list type operation manual are given. The system checkout procedures consist of the software validation, initial hardware checks, and parameter identification flights and are discussed in Section 5.2. General flight test procedures are described in Section 5.3.

5.1 System Operating Procedures

This section describes the operation of the RQAS during research flights. A wiring diagram of the system was given in Figure 3.16 and the control panel layouts in Figure 3.14 and Figure 3.15. A functional description of the switches and indicator lights on both control panels is given in Table 5.1and Table 5.2.

Table 5.1 Pilot Panel switches and indicator lights

Pilot panel:		
S1	Master power switch	Connects 28 VDC to system, closes K0, which connects 115 VAC to system.
S4	Yoke switch	Pilot disengage switch, disconnects power from relays K1 - K4, thereby disengaging actuator signals and hydraulics.
S10	Hydraulic switch	Closes relay K1 if enabled by test engineer hydraulic switch, this opens the shuttle valve.
S12	Signal engage switch	Closes relay K2 if enabled by test engineer signal enable switch, this closes relay K10 which switches computer commands to drive electronics.
L1	Master power	Master power is "ON".
L2	ROLM power	ROLM power is "ON".
L3	DAS power	DAS power is "ON".
L4	Hydraulic	Hydraulic pressure is applied to actuators.
L5	Engage	System is engaged.
L6	Surfaces locked	All RQAS surfaces are locked.

Table 5.2 Engineer panel switches and indicator lights

Engineer Panel:		
S2	ROLM power switch	Switches 115 VAC to ROLM.
S3	DAS power switch	Switches power to DAS.
S6	Disengage switch	Same as yoke switch.
S11	Hydraulic switch	Closes relay K3 which enables pilot's hydraulic switch.
S13	Signal enable switch	Closes relay K4 which enables pilot's signal engage switch.

Both S11 and S13 are normally push to activate, but they also have a 'BYPASS' position in which the switch remains closed, so that the pilot can close them before take-off for pilot only operation.

L11	ROLM power	ROLM power is "ON".
L12	DAS power	DAS power is "ON".
L13	Hydraulic	Hydraulic pressure is applied to the actuators.
L14	Engage	System is engaged.
L15-19	Surfaces locked	Indicates control surface locked, one light for each surface.
L20	Left pump	Left pump pressure is o.k.
L21	Right pump	Right pump pressure is o.k.
L23	Limit switch disengage limit	System has been disengaged by a switch.
L31-42	Limit switches	A limit switch has been triggered, the position of the light on the panel indicates the control surface that reached its limit position.

The engage and disengage sequences are listed below in form of checklists. The normal engage sequence is the sequence used for research flights, on which a test engineer is on board to operate the system.

Normal Engage Sequence

Pilot:	Master power switch	'ON'
Engineer:	ROLM power switch	'ON'
	DAS power switch	'ON'
	Initialize software (handheld terminal)	
	Hydraulics switch - enables pilot 'Hydraulic' switch	'ON'
Pilot:	Hydraulics switch - activates shuttle valve - pressure to RQAS and locking actuat. - surfaces unlock but remain centered - activates 'Hydraulic ON' lights - enables 'Signal engage' switches	'ON'
Engineer:	Signal enable switch - enables pilot 'Signal engage' switch	'Engage'
Pilot:	Signal engage switch - control signals are switched to actuat. - activates 'Engage' indicator lights	'Engage'
Engineer:	Start RQAS software (Handheld Terminal)	

For demonstration flights the monitoring capabilities offered by the test engineer station are not needed, and the system can be operated by the pilot alone. This requires setting some switches on the test enginner panel before take off.

Pilot Only Engage Sequence:

Before Take-off:

Engineer panel:	ROLM power switch	'ON'
	DAS power switch	'ON'
	Hydraulic switch	'Bypass'
	Signal enable switch	'Bypass'
After Take-off:		
Pilot Panel:	Master power switch	'ON'
	Initialize software (Handheld terminal)	
	Hydraulic switch	'ON'
	Signal engage switch	'ON'
	Start RQAS software (Handheld terminal)	

After performing the scheduled research experiments the systems is turned off manually by following the disengage sequence given below:

Disengage Sequence:

Pilot:	Yoke switch	push
or		
Engineer:	Disengage switch	push
	- deactivates relay K10 - actuators get centering signal - deactivates 'Engage' indicator lights - deactivates hydraulic shuttle valve - actuator pressure is released - surfaces center and lock - deactivates 'Hydraulic ON' lights	
Engineer:	DAS power switch	'OFF'
	ROLM power switch	'OFF'
Pilot:	Master power switch	'OFF'

In case of a failure while the system is operating an automatic disengage will take place:

Automatic Disengage:	
Limit switches:	activate relay K12
or	
Computer:	activates relay K11
	- same action as if pilot or test engineer pushes disengage switch.

5.2 System Checkout Procedures

Before the actual flight test program can begin, it must be verified that all system components work properly and that the math models of the airplane used in the controller design are accurate. To this purpose a set of tests including extensive ground checks and parameter identification flights is necessary.

The flight software will be developed and checked using a ground based software verification facility (Figure 5.1). This facility uses a ROLM computer identical to that in the RQAS to ensure that no problems will occur when transferring the software to the actual flight computer. The airplane dynamics and gusts are simulated by a powerful microcomputer containing a non-linear simulation model of the Cessna 402. Pilot commands can be generated with a joystick. The microcomputer sends simulated sensor signals to the ROLM computer and reads the control surface commands that the flight software generates. These can be plotted and analyzed. Errors in the flight software can thus be found. All automatic disengage paths in the software can be checked by sending precomputed signals to the ROLM that will trigger a disengage, e.g. a frozen sensor signal, or a sensor signal out of range. The software

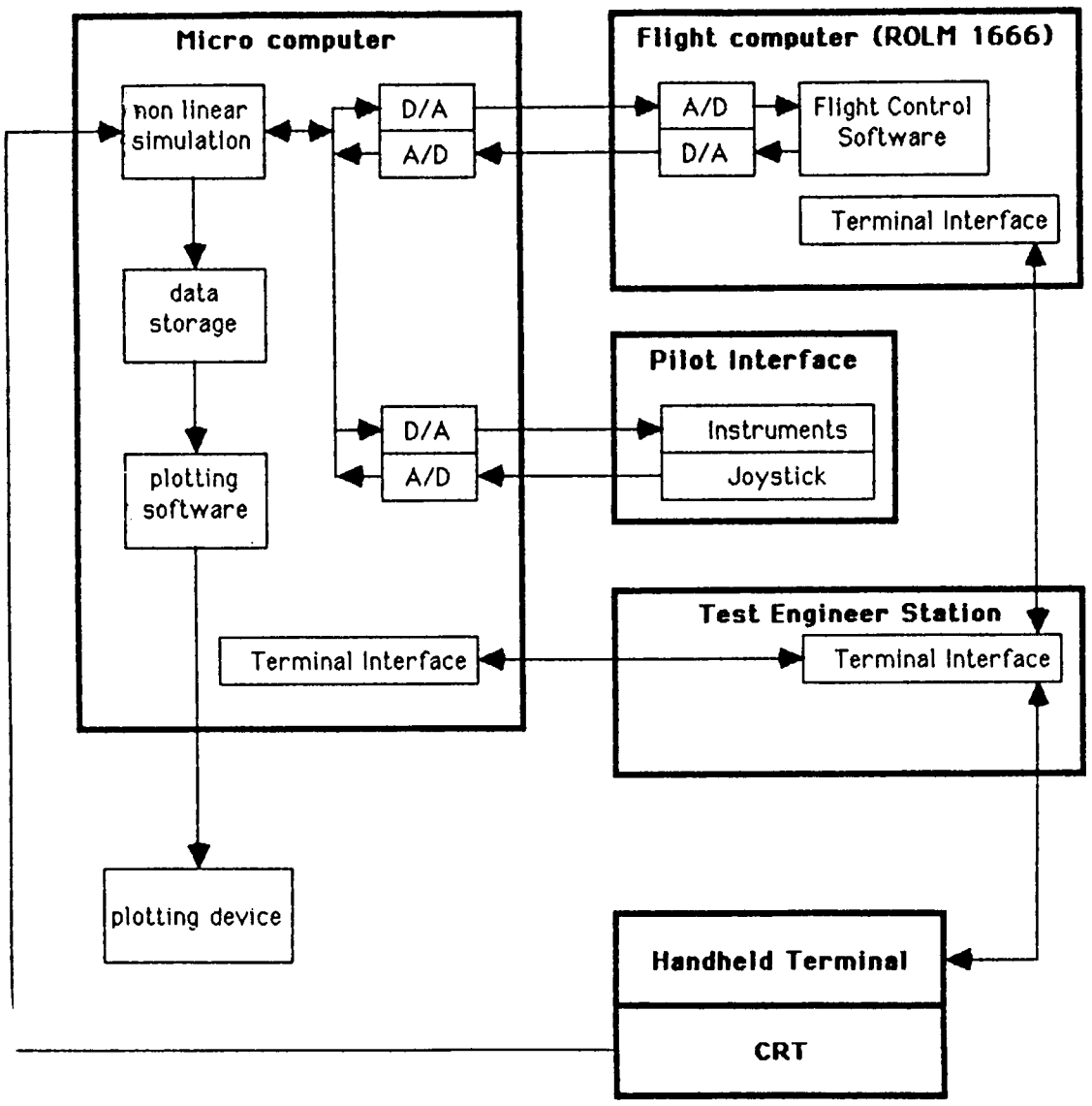

Figure 5.1 Software Verification Facility

verification facility can also be used for preflight checks of the system. In this case it will be connected to the A/D and D/A boards of the ROLM computer in the aircraft. The preflight checkout software has already been described in Section 3.5.5.1.

To ensure the accuracy of the linear math models of the aircraft a set of parameter identification (PI) flights is necessary. The first set of test flights is to verify the airplane stability derivatives and the pilot control derivatives. For these tests the

RQAS surfaces remain centered and locked, and only the DAS system is needed to record the data. Then the RQAS control derivatives must be verified. In this case a special computer program installed in the ROLM computer will send specially designed commands to the dedicated RQAS control surfaces. Again the airplane motion is recorded on the DAS tape. The data are then analyzed using a Modified Maximum Likelihood Estimation (MMLE) program to extract the system matrices.

5.3 General Flight Test Procedures

This section discusses the basic procedures for conducting the RQAS flight test program. Before the first research flight, a flight test plan needs to be established and approved by the proper authorities. This test plan will define the goals and experiments for each test flight. The initial system checkout, parameter identification and software verification must also be completed. A typical test flight follows the procedure outlined below:

- Pilot/Engineer briefing
- C-402B ground check
  - Standard systems
  - Research systems
- Take-off and establish test point

  (RQAS inactive, surfaces locked)
- Execute test plan
- Return to base

  (RQAS inactive, surfaces locked)

- Pilot/Engineer debriefing
- Data processing

The standard system ground check follows the procedures given in the airplane operations manual. The ground check of the research systems is done with the ground check program (Section 3.5.5.1). This program provides an end to end check of all system components including automatic disengage functions. After the ground check the control surfaces will be centered and locked and the rudder servo will be disengaged. The flight test airborne procedure is outlined below:

1. Turn on power to RQAS (Master power, ROLM power, DAS power)
2. Engineer establishes test condition
   - Defines test
   - Monitors sensors and other systems
   - Turns on DAS
3. System is engaged following normal operating procedures (Electrical power is already 'ON')

After test plan is carried out:

4. System is disengaged following normal operating procedures (Electrical power remains 'ON')
5. Engineer turns off DAS
6. Return to step 2. until all planned testing is completed
7. Confirm RQAS control surfaces are centered and locked
8. Turn off electrical power

6 Conclusions

This report documents the detailed design of a ride quality augmentation system for commuter aircraft. The system is designed to be installed in a Cessna 402B aircraft, an 8 passenger twin. The hardware modifications have been designed by Cessna aircraft in Wichita, KS, under subcontract to KU-FRL, with detailed design drawings completed. The design includes the detailed design of the control surfaces, the hydraulic system, and the selection of the actuators. The actuators are undergoing tests to establish flight worthiness at NASA LaRC. The instrumentation system, which consists of the ROLM flight computer, a sensor package, data recording system, and the pilot and test engineer control panel, was designed by NASA LaRC. The overall system design and the flight software was developed at KU-FRL. At this point the software has not been programmed, but all sub-programs are well defined and discussed in this report.

The RQAS is shown to perform well by means of linear simulations and power spectral densities. Either analysis method shows a reduction in $\bar{a}_z$ of between 40% and 50% of the open loop acceleration plus an equally strong reduction in $\bar{a}_y$. However, the RQAS increases longitudinal acceleration, but its magnitude remains small. The power spectral density plots show that the RQAS achieves the largest reduction of accelerations in the frequency range from 0.1 to 3 rad/sec, which is the frequency at which passengers are most likely to suffer from motion sickness. The maneuvering algorithm has performed well in linear simulation. It is recognized that the command model is only an approximation of the real airplane, the augmented airplane will show basicly the same dynamic behaviour as the command model. Therefore the characteristics of the airplane may be altered somewhat when the RQAS is operating.

At this point the following tasks remain to fully complete the RQAS project:

1. Program the software
2. Build the hardware
3. Install the system in the airplane
4. Define a flght test plan
5. Carry out flight test plan
6. Document final results.

References

1. Downing, D. R.; Hammond, T. A.; and Amin, S. P.: "Ride Quality Systems for Commuter Aircraft." NASA CR-166118, May 1983.

2. Hammond, T. A.; Amin, S. P.; Paduana, J.; and Downing, D. R.: "Design of a Digital Ride Quality Augmentation System for Commuter Aircraft." NASA CR-172419, October 1984.

3. Davis, D. J.; Linse, D. J.; Suikat, R.; Entz, D. P.: "Preliminary Control Law and Hardware Designs for a Ride Quality Augmentation System for Commuter Aircraft." NASA CR-4014, September 1986.

4. MIL-F-8785C (ASG) Military Specifications: Flying Qualities of Piloted Airplanes, August 1969.

5. Richards, L. G.; Kuhltau, A. R.; Jacobson, I. D.: "Passenger Ride Quality Determined From Commercial Airline Flights." 1975 Ride Quality Symposium. NASA TM X-3295, DOT-TSC-OST-75-40, 1975, pp. 409-436.

6. Holloway, R. D.; Thompson, G. O.; Rohling, W. J.: "Prospect for Low Wing Loading STOL Transports with Ride Smoothing." Journal of Aircraft, Vol. 9, No. 8, August 1972.

7. Roskam, J.: "Airplane Flight Dynamics and Automatic Controls," Parts I and II, Roskam Aviation and Engineering Corp., Ottawa, KS, 1982.

8. Davis, D. J.: "A Comparison of Two Optimal Regulator Design Techniques for the Weighting of Output Variables which are Linear Combinations of States and Controls." Master's Thesis, University of Kansas, 1986.

9. Dorato, P.; and Louis, A. H.: "Optimal Linear Regulators: The Discrete Time Case." IEEE Trans. Auto Control, Vol. AC-16, No. 6, Dec. 1971.

10. CTRL-C, Systems Control Technology, Inc., Version 4.0, Sept. 1986.

11. "Interactive Control Augmentation Design," University of Kansas Center for Research, Inc., 1985.

12. Heath, R. E.: "State Variable Model of Windgusts." AFFDL/FGC-TM-72, 1982.

13. Boehret, H.; and Krag, B.: OLGA, an Open Loop Gust Alleviation System, AGARD CP-384.

Appendix A Mathematical Models for the Cessna 402B

This appendix presents the basic math model of the Cessna 402B. These are linearizations about the trim points specified in Table 2.2 of the NASA LaRC nonlinear simulation model of the airplane. The models are presented in form of the four basic matrices which satisfy the following linearized equations:

For the longitudinal models:

$$\begin{bmatrix} \dot{\alpha} \\ \dot{u} \\ \dot{q} \\ \dot{\theta} \end{bmatrix} = \begin{bmatrix} A_{11} & A_{12} & A_{13} & A_{14} \\ A_{21} & A_{22} & A_{23} & A_{24} \\ A_{31} & A_{32} & A_{33} & A_{34} \\ A_{41} & A_{42} & A_{43} & A_{44} \end{bmatrix} \begin{bmatrix} \alpha \\ u \\ q \\ \theta \end{bmatrix} + \begin{bmatrix} B_{11} & B_{12} \\ B_{21} & B_{22} \\ B_{31} & B_{32} \\ B_{41} & B_{42} \end{bmatrix} \begin{bmatrix} \delta_{se} \\ \delta_f \end{bmatrix}$$

$$\begin{bmatrix} a_z \\ a_x \\ \alpha \\ u \\ q \\ \theta \end{bmatrix} = \begin{bmatrix} C_{11} & C_{12} & C_{13} & C_{14} \\ C_{21} & C_{22} & C_{23} & C_{24} \\ C_{31} & C_{32} & C_{33} & C_{34} \\ C_{41} & C_{42} & C_{43} & C_{44} \\ C_{51} & C_{52} & C_{53} & C_{54} \\ C_{61} & C_{62} & C_{63} & C_{64} \end{bmatrix} \begin{bmatrix} \alpha \\ u \\ q \\ \theta \end{bmatrix} + \begin{bmatrix} D_{11} & D_{12} \\ D_{21} & D_{22} \\ D_{31} & D_{32} \\ D_{41} & D_{42} \\ D_{51} & D_{52} \\ D_{61} & D_{62} \end{bmatrix} \begin{bmatrix} \delta_{se} \\ \delta_f \end{bmatrix}$$

For the lateral directional models:

$$\begin{bmatrix} \dot{\beta} \\ \dot{p} \\ \dot{r} \\ \dot{\phi} \end{bmatrix} = \begin{bmatrix} A_{11} & A_{12} & A_{13} & A_{14} \\ A_{21} & A_{22} & A_{23} & A_{24} \\ A_{31} & A_{32} & A_{33} & A_{34} \\ A_{41} & A_{42} & A_{43} & A_{44} \end{bmatrix} \begin{bmatrix} \beta \\ p \\ r \\ \phi \end{bmatrix} + \begin{bmatrix} B_{11} & B_{12} \\ B_{21} & B_{22} \\ B_{31} & B_{32} \\ B_{41} & B_{42} \end{bmatrix} \begin{bmatrix} \delta_{df} \\ \delta_r \end{bmatrix}$$

$$\begin{bmatrix} a_y \\ \beta \\ p \\ r \\ \phi \end{bmatrix} = \begin{bmatrix} C_{11} & C_{12} & C_{13} & C_{14} \\ C_{21} & C_{22} & C_{23} & C_{24} \\ C_{31} & C_{32} & C_{33} & C_{34} \\ C_{41} & C_{42} & C_{43} & C_{44} \\ C_{51} & C_{52} & C_{53} & C_{54} \end{bmatrix} \begin{bmatrix} \beta \\ p \\ r \\ \phi \end{bmatrix} + \begin{bmatrix} D_{11} & D_{12} \\ D_{21} & D_{22} \\ D_{31} & D_{32} \\ D_{41} & D_{42} \\ D_{51} & D_{52} \end{bmatrix} \begin{bmatrix} \delta_{df} \\ \delta_r \end{bmatrix}$$

Table A.1 Longitudinal Model for Sea Level Take-Off

$$A = \begin{bmatrix} -1.1730 & -0.0017 & 0.9133 & -0.0249 \\ 9.6588 & -0.0278 & 0.0000 & -31.7843 \\ -5.4978 & 0.0007 & -7.5327 & 0.0784 \\ 0.0000 & 0.0000 & 1.0000 & 0.0000 \end{bmatrix}$$

$$B = \begin{bmatrix} -0.0361 & -0.2487 \\ 0.0000 & -4.5082 \\ -3.7650 & 1.1163 \\ 0.0000 & 0.0000 \end{bmatrix}$$

$$C = \begin{bmatrix} -215.670 & -0.3190 & -14.4151 & 3.8725 \\ 9.6588 & -0.0278 & 21.6076 & -0.7103 \\ 1.0000 & 0.0000 & 0.0000 & 0.0000 \\ 0.0000 & 1.0000 & 0.0000 & 0.0000 \\ 0.0000 & 0.0000 & 1.0000 & 0.0000 \\ 0.0000 & 0.0000 & 0.0000 & 1.0000 \end{bmatrix}$$

$$D = \begin{bmatrix} -6.6301 & -41.5912 \\ 0.0000 & -4.5082 \\ 0.0000 & 0.0000 \\ 0.0000 & 0.0000 \\ 0.0000 & 0.0000 \\ 0.0000 & 0.0000 \end{bmatrix}$$

Table A.2 Longitudinal Model for Sea Level Climb

$$A = \begin{bmatrix} -1.3325 & -0.0014 & 0.9189 & -0.0120 \\ 12.7885 & -0.0228 & 0.0000 & -32.0688 \\ -6.4781 & 0.0023 & -8.1525 & 0.0406 \\ 0.0000 & 0.0000 & 1.0000 & 0.0000 \end{bmatrix}$$

$$B = \begin{bmatrix} -0.0389 & -0.2853 \\ 0.0000 & -5.9288 \\ -4.6678 & 1.4135 \\ 0.0000 & 0.0000 \end{bmatrix}$$

$$C = \begin{bmatrix} -280.959 & -0.2952 & -16.2570 & 2.8658 \\ 12.7885 & -0.0228 & 17.8530 & -0.3242 \\ 1.0000 & 0.0000 & 0.0000 & 0.0000 \\ 0.0000 & 1.0000 & 0.0000 & 0.0000 \\ 0.0000 & 0.0000 & 1.0000 & 0.0000 \\ 0.0000 & 0.0000 & 0.0000 & 1.0000 \end{bmatrix}$$

$$D = \begin{bmatrix} -8.2010 & -54.7130 \\ 0.0000 & -5.9354 \\ 0.0000 & 0.0000 \\ 0.0000 & 0.0000 \\ 0.0000 & 0.0000 \\ 0.0000 & 0.0000 \end{bmatrix}$$

Table A.3 Longitudinal Model for 5,000 ft Climb

$$A = \begin{bmatrix} -1.2413 & -0.0012 & 0.9304 & -0.0105 \\ 12.5650 & -0.2120 & 0.0000 & -32.0750 \\ -7.1464 & 0.0016 & -7.5786 & 0.0330 \\ 0.0000 & 0.0000 & 1.0000 & 0.0000 \end{bmatrix}$$

$$B = \begin{bmatrix} -0.0361 & -0.2650 \\ 0.0000 & -5.9288 \\ -4.6749 & 1.2914 \\ 0.0000 & 0.0000 \end{bmatrix}$$

$$C = \begin{bmatrix} -282.200 & -0.2662 & -14.9489 & 2.8681 \\ 12.5650 & -0.0212 & 19.9067 & -0.3061 \\ 1.0000 & 0.0000 & 0.0000 & 0.0000 \\ 0.0000 & 1.0000 & 0.0000 & 0.0000 \\ 0.0000 & 0.0000 & 1.0000 & 0.0000 \\ 0.0000 & 0.0000 & 0.0000 & 1.0000 \end{bmatrix}$$

$$D = \begin{bmatrix} -8.2155 & -54.9407 \\ 0.0000 & -5.9354 \\ 0.0000 & 0.0000 \\ 0.0000 & 0.0000 \\ 0.0000 & 0.0000 \\ 0.0000 & 0.0000 \end{bmatrix}$$

Table A.4 Longitudinal Model for 20,000 ft Climb

$$A = \begin{bmatrix} -1.2343 & -0.0005 & 0.9583 & 0.0000 \\ 18.3366 & -0.0178 & 0.0000 & -32.1733 \\ -11.7142 & 0.0008 & -7.1964 & 0.0000 \\ 0.0000 & 0.0000 & 1.0000 & 0.0000 \end{bmatrix}$$

$$B = \begin{bmatrix} -0.0343 & -0.2642 \\ 0.0000 & -9.2631 \\ -6.9711 & 1.5455 \\ 0.0000 & 0.0000 \end{bmatrix}$$

$$C = \begin{bmatrix} -441.787 & -0.1736 & -14.4977 & 1.5504 \\ 18.3366 & -0.0178 & 17.2334 & -0.0107 \\ 1.0000 & 0.0000 & 0.0000 & 0.0000 \\ 0.0000 & 1.0000 & 0.0000 & 0.0000 \\ 0.0000 & 0.0000 & 1.0000 & 0.0000 \\ 0.0000 & 0.0000 & 0.0000 & 1.0000 \end{bmatrix}$$

$$D = \begin{bmatrix} -12.2596 & -86.7313 \\ 0.0000 & -9.2750 \\ 0.0000 & 0.0000 \\ 0.0000 & 0.0000 \\ 0.0000 & 0.0000 \\ 0.0000 & 0.0000 \end{bmatrix}$$

Table A.5 Longitudinal Model for Sea Level Approach

$$A = \begin{bmatrix} -1.1854 & -0.0019 & 0.9181 & 0.0089 \\ 9.9493 & -0.0359 & 0.0000 & -32.1271 \\ -5.8824 & 0.0043 & -6.7588 & -0.0253 \\ 0.0000 & 0.0000 & 1.0000 & 0.0000 \end{bmatrix}$$

$$B = \begin{bmatrix} -0.0323 & -0.2504 \\ 0.0000 & -4.4972 \\ -3.3467 & 1.0004 \\ 0.0000 & 0.0000 \end{bmatrix}$$

$$C = \begin{bmatrix} -215.939 & -0.3383 & -13.3899 & -4.1126 \\ 9.9493 & -0.0359 & 23.5067 & -0.0075 \\ 1.0000 & 0.0000 & 0.0000 & 0.0000 \\ 0.0000 & 1.0000 & 0.0000 & 0.0000 \\ 0.0000 & 0.0000 & 1.0000 & 0.0000 \\ 0.0000 & 0.0000 & 0.0000 & 1.0000 \end{bmatrix}$$

$$D = \begin{bmatrix} -5.8771 & -41.5288 \\ 0.0000 & 4.5000 \\ 0.0000 & 0.0000 \\ 0.0000 & 0.0000 \\ 0.0000 & 0.0000 \\ 0.0000 & 0.0000 \end{bmatrix}$$

Table A.6 Lateral Model for Sea Level Take-Off

$$\mathbf{A} = \begin{bmatrix} -0.1547 & 0.1178 & -0.9939 & 0.1688 \\ -2.9322 & -2.4155 & 0.3692 & -0.0062 \\ 2.5862 & -0.3308 & -0.3206 & -0.0063 \\ 0.0000 & 1.0000 & 0.2716 & 0.0000 \end{bmatrix}$$

$$\mathbf{B} = \begin{bmatrix} -0.0055 & 0.4178 \\ -2.1990 & 0.7562 \\ -0.0912 & -1.5865 \\ 0.0000 & 0.0000 \end{bmatrix}$$

$$\mathbf{C} = \begin{bmatrix} -28.4455 & 0.4673 & -0.3944 & -0.0424 \\ 1.0000 & 0.0000 & 0.0000 & 0.0000 \\ 0.0000 & 1.0000 & 0.0000 & 0.0000 \\ 0.0000 & 0.0000 & 1.0000 & 0.0000 \\ 0.0000 & 0.0000 & 0.0000 & 1.0000 \end{bmatrix}$$

$$\mathbf{D} = \begin{bmatrix} 0.0000 & 7.6819 \\ 0.0000 & 0.0000 \\ 0.0000 & 0.0000 \\ 0.0000 & 0.0000 \\ 0.0000 & 0.0000 \end{bmatrix}$$

C-2

Table A.7 Lateral Model for Sea Level Climb

$$\mathbf{A} = \begin{bmatrix} -0.1879 & 0.0874 & -0.9971 & 0.1505 \\ -3.7107 & -2.6275 & 0.3918 & -0.0070 \\ 3.7138 & -0.2901 & -0.3503 & -0.0065 \\ 0.0000 & 1.0000 & 0.1700 & 0.0000 \end{bmatrix}$$

$$\mathbf{B} = \begin{bmatrix} -0.0063 & 0.0486 \\ -3.8947 & 1.0087 \\ -0.0906 & -2.1043 \\ 0.0000 & 0.0000 \end{bmatrix}$$

$$\mathbf{C} = \begin{bmatrix} -39.6290 & 0.0203 & -0.2305 & -0.0067 \\ 1.0000 & 0.0000 & 0.0000 & 0.0000 \\ 0.0000 & 1.0000 & 0.0000 & 0.0000 \\ 0.0000 & 0.0000 & 1.0000 & 0.0000 \\ 0.0000 & 0.0000 & 0.0000 & 1.0000 \end{bmatrix}$$

$$\mathbf{D} = \begin{bmatrix} 0.0000 & 10.2398 \\ 0.0000 & 0.0000 \\ 0.0000 & 0.0000 \\ 0.0000 & 0.0000 \\ 0.0000 & 0.0000 \end{bmatrix}$$

Table A.8 Lateral Model for 5,000ft Climb

$$\mathbf{A} = \begin{bmatrix} -0.1742 & 0.0876 & -0.9969 & 0.1397 \\ -3.7132 & -2.4327 & 0.3639 & -0.0060 \\ 3.7107 & -0.2692 & -0.3246 & -0.0056 \\ 0.0000 & 1.0000 & 0.1653 & 0.0000 \end{bmatrix}$$

$$\mathbf{B} = \begin{bmatrix} -0.0059 & 0.0450 \\ -3.8943 & 1.0089 \\ -0.0908 & -2.1036 \\ 0.0000 & 0.0000 \end{bmatrix}$$

$$\mathbf{C} = \begin{bmatrix} -39.6099 & 0.0192 & -0.2173 & -0.0103 \\ 1.0000 & 0.0000 & 0.0000 & 0.0000 \\ 0.0000 & 1.0000 & 0.0000 & 0.0000 \\ 0.0000 & 0.0000 & 1.0000 & 0.0000 \\ 0.0000 & 0.0000 & 0.0000 & 1.0000 \end{bmatrix}$$

$$\mathbf{D} = \begin{bmatrix} 0.0000 & 10.2390 \\ 0.0000 & 0.0000 \\ 0.0000 & 0.0000 \\ 0.0000 & 0.0000 \\ 0.0000 & 0.0000 \end{bmatrix}$$

Table A.9 Lateral Model for 20,000 ft Cruise

$$A = \begin{bmatrix} -0.1843 & 0.0482 & -0.9993 & 0.0898 \\ -5.3309 & -2.3284 & 0.3048 & -0.0039 \\ 6.3295 & -0.1677 & -0.3141 & -0.0032 \\ 0.0000 & 1.0000 & 0.0482 & 0.0000 \end{bmatrix}$$

$$B = \begin{bmatrix} -0.0058 & 0.0454 \\ -6.1662 & 1.5993 \\ -0.0645 & -3.3271 \\ 0.0000 & 0.0000 \end{bmatrix}$$

$$C = \begin{bmatrix} -65.9673 & 0.0083 & -0.1746 & -0.0156 \\ 1.0000 & 0.0000 & 0.0000 & 0.0000 \\ 0.0000 & 1.0000 & 0.0000 & 0.0000 \\ 0.0000 & 0.0000 & 1.0000 & 0.0000 \\ 0.0000 & 0.0000 & 0.0000 & 1.0000 \end{bmatrix}$$

$$D = \begin{bmatrix} 0.0000 & 16.2600 \\ 0.0000 & 0.0000 \\ 0.0000 & 0.0000 \\ 0.0000 & 0.0000 \\ 0.0000 & 0.0000 \end{bmatrix}$$

Table A.10 Lateral Model for Sea Level Approach

$$\mathbf{A} = \begin{bmatrix} -0.1452 & 0.0871 & -0.9971 & 0.2008 \\ -2.1765 & -2.0130 & 0.3034 & -0.0072 \\ 2.1817 & -0.2224 & -0.2692 & -0.0067 \\ 0.0000 & 1.0000 & 0.0348 & 0.0000 \end{bmatrix}$$

$$\mathbf{B} = \begin{bmatrix} -0.0056 & 0.0419 \\ -2.8866 & 0.7502 \\ -0.0988 & -1.5782 \\ 0.0000 & 0.0000 \end{bmatrix}$$

$$\mathbf{C} = \begin{bmatrix} -27.8097 & 0.0224 & -0.1667 & -0.0021 \\ 1.0000 & 0.0000 & 0.0000 & 0.0000 \\ 0.0000 & 1.0000 & 0.0000 & 0.0000 \\ 0.0000 & 0.0000 & 1.0000 & 0.0000 \\ 0.0000 & 0.0000 & 0.0000 & 1.0000 \end{bmatrix}$$

$$\mathbf{D} = \begin{bmatrix} 0.0000 & 7.6297 \\ 0.0000 & 0.0000 \\ 0.0000 & 0.0000 \\ 0.0000 & 0.0000 \\ 0.0000 & 0.0000 \end{bmatrix}$$

Appendix B Controller Gain Tables

The feedback gains for both the output weighting and the control rate weighting designs are listed in this appendix.

Output Weighting

In this case the system is given by:

$$\dot{\mathbf{x}} = \mathbf{Ax} + \mathbf{Bu}$$

$$\mathbf{y} = \mathbf{Cx} + \mathbf{Du}$$

and the control law is

$$\mathbf{u} = -\mathbf{Kx}$$

The diagonal elements of the weighting matrices used in the controller designs are for the longitudinal case:

Q = diag(0.2, 10.0, 0.0001, 15.0, 20.0),

R = diag(15.0, 8.0),

and for the lateral case:

Q = diag(0.01, 15.0, 0.07, 0.5, 1.5),

R = diag(3.0, 5.5).

The resulting gain matrices are listed below.

Sea level take-off:

$$K_{long} = \begin{bmatrix} -0.1555 & -0.0011 & -0.4102 & -1.3472 \\ 3.9699 & 0.0061 & 0.3850 & 0.7320 \end{bmatrix}$$

$$K_{lat} = \begin{bmatrix} -0.2406 & -0.2959 & 0.0877 & -0.7487 \\ 0.4864 & 0.0917 & -0.8192 & 0.0092 \end{bmatrix}$$

Sea level climb:

$$K_{long} = \begin{bmatrix} -0.7054 & -0.0016 & -0.4195 & -0.8162 \\ 4.2135 & 0.0045 & 0.3406 & 0.4978 \end{bmatrix}$$

$$K_{lat} = \begin{bmatrix} -0.1336 & -0.2592 & 0.0808 & -0.7277 \\ 0.4213 & 0.0756 & -0.8136 & 0.0282 \end{bmatrix}$$

5,000 ft climb:

$$K_{long} = \begin{bmatrix} -0.7043 & -0.0014 & -0.4477 & -0.8054 \\ 4.2297 & 0.0040 & 0.3261 & 0.4979 \end{bmatrix}$$

$$K_{lat} = \begin{bmatrix} -0.1152 & -0.2707 & 0.0710 & -0.7220 \\ 0.4291 & 0.0748 & -0.8317 & 0.0236 \end{bmatrix}$$

20,000 ft cruise:

$$K_{long} = \begin{bmatrix} -1.4238 & -0.0015 & -0.5531 & -0.0841 \\ 4.5300 & 0.0018 & 0.2505 & 0.2413 \end{bmatrix}$$

$$K_{lat} = \begin{bmatrix} 0.1169 & -0.2501 & 0.0182 & -0.6980 \\ 0.3153 & 0.0475 & -0.8796 & 0.0269 \end{bmatrix}$$

Sea level approach:

$$K_{long} = \begin{bmatrix} -0.6915 & -0.0023 & -0.4199 & -0.7079 \\ 4.1620 & 0.0068 & 0.3618 & 0.5073 \end{bmatrix}$$

$$K_{lat} = \begin{bmatrix} -0.1581 & -0.3075 & 0.1333 & -0.7273 \\ 0.5175 & 0.1078 & -0.8262 & 0.0298 \end{bmatrix}$$

For the control rate weighting design, the airplane model is augmented by the controls. Therefore the control positions need to be fed back and the commanded variable is actually the control rate. The system is now given by:

$$\begin{bmatrix} \dot{x} \\ \dot{u} \end{bmatrix} = \begin{bmatrix} A & B \\ 0 & 0 \end{bmatrix} \begin{bmatrix} x \\ u \end{bmatrix} + \begin{bmatrix} 0 \\ I \end{bmatrix} \dot{u}$$

Therefore the gain matrices are now (6x2) matrices. An additional weighting matrix, S, is used to weight the control rates. This matrix is in the longitudinal case:

S = diag(0.2, 0.06)

and in the lateral case:

S = diag(0.007, 0.1).

The resulting gains are listed below:

Sea level take-off:

K_{long} =

$$\begin{bmatrix} 6.9342 & 0.0010 & -11.8300 & -10.0002 & 9.3337 & 1.2952 \\ 165.4630 & 0.2534 & 15.3368 & 25.0176 & 3.5424 & 42.5702 \end{bmatrix}$$

K_{lat} =

$$\begin{bmatrix} -3.2907 & -5.2223 & 2.1000 & -12.8389 & 17.9367 & -1.2261 \\ 1.2343 & 0.7131 & -5.9113 & 0.0525 & -0.1046 & 8.5173 \end{bmatrix}$$

Sea level climb:

K_{long} =

$$\begin{bmatrix} 4.9010 & -0.0019 & -1.7849 & -7.0164 & 9.5752 & 1.4239 \\ 186.1556 & 0.1881 & 15.0129 & 27.9389 & 3.8274 & 47.5861 \end{bmatrix}$$

K_{lat} =

$$\begin{bmatrix} -1.3268 & -4.5976 & 2.1941 & -12.4973 & 18.1029 & -1.5929 \\ 0.1345 & 0.6058 & -5.9621 & 0.1803 & -0.1329 & 9.1020 \end{bmatrix}$$

5,000 ft climb

K_{long} =

$$\begin{bmatrix} 5.1959 & -0.0013 & -2.0041 & -6.8620 & 9.6803 & 1.4273 \\ 186.6549 & 0.1654 & 14.3496 & 28.4334 & 3.9006 & 47.6253 \end{bmatrix}$$

K_{lat} =

$$\begin{bmatrix} -1.0165 & -4.8023 & 2.0320 & -12.3906 & 18.1481 & -1.5686 \\ 0.1341 & 0.6045 & -6.1194 & 0.1492 & -0.1308 & 9.1384 \end{bmatrix}$$

20,000 ft cruise

K_{long}=

$$\begin{bmatrix} 1.6775 & -0.0090 & -2.5466 & -0.2951 & 10.7246 & 1.5887 \\ 235.4188 & 0.0898 & 11.8217 & 12.6984 & 4.3890 & 54.2403 \end{bmatrix}$$

K_{lat} =

$$\begin{bmatrix} 3.0680 & -4.4882 & 1.7708 & -12.0213 & 18.6970 & -2.4028 \\ -2.3969 & 0.4325 & -7.0218 & 0.2078 & -0.1917 & 10.8652 \end{bmatrix}$$

Sea level approach

K_{long}=

$$\begin{bmatrix} 2.4345 & -0.0097 & -2.0035 & -5.0973 & 9.2045 & 1.1769 \\ 171.2851 & 0.2763 & 14.7118 & 18.6669 & 3.2227 & 42.4638 \end{bmatrix}$$

K_{lat} =

$$\begin{bmatrix} -1.7939 & -5.4593 & 2.9971 & -12.4815 & 17.9604 & -1.4069 \\ 1.4688 & 0.8396 & -5.9780 & 0.1964 & -0.1208 & 8.5298 \end{bmatrix}$$

Appendix C RQAS wiring diagram parts list

Table C.1 RQAS Switch Designations

S1	main power switch	pilot's panel
S2	ROLM power switch	engineer's panel
S3	DAS power switch	engineer's panel
S4	pilot disengage	yoke
S6	engineer disengage	engineer's panel
S10	hydraulic	pilot's panel
S11	hydraulic enable	engineer's panel
S12	signal engage	pilot's panel
S13	signal enable	engineer's panel
SL1-10	limit switches	control surfaces

Table C.2 RQAS Indicator Lights

L1	main power	pilot's panel	green
L2	ROLM power	"	green
L3	DAS power	"	green
L4	hydraulic pressure	"	green
L5	signal engage	"	green
L6	surfaces locked	"	green
L11	ROLM power	engineer's panel	green
L12	DAS power	"	green
L13	hydraulic pressure	"	green
L14	signal engage	"	green
L15	LO flap locked	"	green
L16	LI flap locked	"	green
L17	RI flap locked	"	green
L18	RO flap locked	"	green
L19	sep. elevator locked	"	green
L20	left pump pressure	"	green
L21	right pump pressure	"	green
L23	limit switch diseng.	"	red
L31	LO upper limit	"	red
L32	LO lower limit	"	red
L33	LI upper limit	"	red
L34	LI lower limit	"	red
L35	RI upper limit	"	red
L36	RI lower limit	"	red
L37	RO upper limit	"	red
L38	RO lower limit	"	red
L39	sep elev. upper limit	"	red
L40	sep elev. lower limit	"	red

Table C.3 RQAS Connectors

J1	Hyd. valve, V1, to terminal strip, T6
J2	Actuator switch, SP1, to terminal strip, T6
J3	Right pump pressure, SP2, to terminal strip, T6
J4	Left pump pressure, SP3, to terminal strip, T6
J5	LO servo to terminal strip, T1
J6	LI servo to terminal strip, T2
J7	RI servo to terminal strip, T3
J8	RO servo to terminal strip, T4
J9	SE servo to terminal strip, T5
J10	LO LVDT to terminal strip, T1
J11	LI LVDT to terminal strip, T2
J12	RI LVDT to terminal strip, T3
J13	RO LVDT to terminal strip, T4
J14	SE LVDT to terminal strip, T5
J15	LO locking actuator to terminal strip, T1
J16	LI locking actuator to terminal strip, T2
J17	RI locking actuator to terminal strip, T3
J18	RO locking actuator to terminal strip, T4
J19	SE locking actuator to terminal strip, T5
J22	Pilot panel to 115 VAC
J23	Pilot panel to 28 VDC
J24	Engineer panel to signal conditioner
J25	Engineer panel to Cessna interface (T1-T6)
J26	Engineer panel to handheld terminal (RS 232)
J27	Engineer panel to ROLM (not shown)
J28	Engineer panel to DAS (not shown)
J29	Engineer panel to relay box
J30	Engineer panel to ROLM (RS 232, for handheld terminal)
J31	Engineer panel to pilot panel
J32	Pilot panel to Engineer panel
J33	Pilot panel to yoke switch
J34	Meter signal conditioner to engineer panel
J35	Meter signal conditioner to drive electronics
J36	Drive electronics to meter signal conditioner
J37	Drive electronic to Cessna interface (T1-T6)
J38	Drive electronics LVDT signals to ROLM
J39	Drive electronics commands from relay box
J40	Relay box to engineer panel
J42	Relay box to drive electronics
J43	Relay box to rudder
J44	Relay box to DAS
J45	Relay box to ROLM
J47	ROLM RS 232 to engineer panel
J48	ROLM commands to relay box
J50	ROLM LVDT signals from drive electronics

Table C.4 RQAS Terminal Strips

T1	Left Outboard Flap
T2	Left Inboard Flap
T3	Right Inboard Flap
T4	Right Outboard Flap
T5	Separate Surface Elevator
T6	Hydraulic System

Table C.5 RQAS Relays

K0	pilot panel 115 VAC
K1	pilot panel hydraulic
K2	pilot panel signal engage
K3	engineer panel hydraulic
K4	engineer panel signal engage
K10	signal engage (relay box)
K11	computer disengage
K12	limit switch disengage
K13	DAS power

Appendix D Open and Closed Loop Eigenvalues

Table D.1 Eigenvalues for Flight Condition 1

	Z-Domain		S-Domain		Freq.	Damping
	Real	Imag	Real	Imag	Rad/sec	
Open Loop Longitudinal			-0.0034	0.1516	0.1516	0.0226
			-0.0034	-0.1516	(phugoid)	
			-2.1087	0.0000		
			-6.6180	0.0000		
OW Longitudinal	0.9987	0.0006	-0.0667	0.0292	0.0728	0.9160
	0.9987	-0.0006	-0.0667	-0.0292		
	0.9522	0.0000	-2.4495	0.0000		
	0.8607	0.0477	-7.4229	2.7673	7.9219	0.9370
	0.8607	-0.0477	-7.4229	-2.7673		
	0.7993	0.0000	-11.2001	0.0000		
CRW Longitudinal	0.9987	0.0006	-0.0667	0.0292	0.0728	0.9158
	0.9987	-0.0006	-0.0667	-0.0292		
	0.9505	0.0000	-2.5404	0.0000		
	0.8918	0.0459	-5.6596	2.5725	6.2168	0.9104
	0.8918	-0.0459	-5.6596	-2.5725		
	0.7957	0.0000	-11.4271	0.0000		
	0.7589	0.0000	-13.7912	0.0000		
	0.1479	0.0000	-95.5493	0.0000		
Open Loop Lateral			0.0377	0.0000		
			-0.2352	1.7726	1.7882	0.1316
			-0.2352	-1.7726	(dutch roll)	
			-2.4581	0.0000		
OW Lateral	0.9828	0.0000	-0.8673	0.0000		
	0.9779	0.0394	-1.0785	2.0256	2.2948	0.4700
	0.9779	-0.0394	-1.0785	-2.0256		
	0.9545	0.0000	-2.3291	0.0000		
	0.8494	0.0000	-8.1627	0.0000		
	0.8330	0.0000	-9.1353	0.0000		
CRW Lateral	0.9827	0.0000	-0.8739	0.0000		
	0.9546	0.0000	-2.3247	0.0000		
	0.9787	0.0410	-1.0344	2.0944	2.3359	0.4428
	0.9787	-0.0410	-1.0344	-2.0944		
	0.9075	0.0000	-4.8532	0.0000		
	0.8475	0.0000	-8.2757	0.0000		
	0.7725	0.0000	-12.9030	0.000		
	0.6284	0.0000	-23.2253	0.0000		

Table D.2 Eigenvalues for Flight Condition 2

	Z-Domain		S-Domain		Freq.	Damping
	Real	Imag	Real	Imag	Rad/sec	
Open Loop Longitudinal			-0.0067	0.1511	0.1513	0.0443
			-0.0067	-1.1511	(phugoid)	
			-2.3646	0.0000		
			-7.1298	0.0000		
OW Longitudinal	0.9989	0.0007	-0.0552	0.0352	0.0654	0.8437
	0.9989	0.0007	-0.0552	-0.0352		
	0.9499	0.0000	-2.5762	0.0000		
	0.8570	0.0622	-7.5854	3.6233	8.4063	0.9023
	0.8570	-0.0622	-7.5854	-3.6233		
	0.7943	0.0000	-11.5150	0.0000		
CRW Longitudinal	0.9984	0.0007	-0.0800	0.0354	0.0875	0.9143
	0.9984	-0.0007	-0.0800	-0.0354		
	0.9476	0.0000	-2.6910	0.0000		
	0.8905	0.0548	-5.7019	3.0732	6.4770	0.8803
	0.8905	-0.0548	-5.7019	-3.0732		
	0.7924	0.0000	-11.6131	0.0000		
	0.7496	0.0000	-14.4099	0.0000		
	0.0473	0.0000	-152.552	0.0000		
Open Loop Lateral			0.0215	0.0000		
			-0.2560	2.0646	2.0804	0.1230
			-0.2560	-20.646	(dutch roll)	
			-2.6753	0.0000		
OW Lateral	0.9776	0.0000	-1.1340	0.0000		
	0.9519	0.0000	-2.4652	0.0000		
	0.9712	0.0454	-1.4075	2.3372	2.7282	0.5159
	0.9712	-0.0454	-1.4075	-2.3372		
	0.8605	0.0000	-7.5104	0.0000		
	0.8363	0.0000	-8.9412	0.0000		
CRW Lateral	0.9773	0.0000	-1.1484	0.0000		
	0.9521	0.0000	-2.4526	0.0000		
	0.9728	0.0485	-1.3147	2.4901	2.8159	0.4669
	0.9728	-0.0485	-1.3147	-2.4901		
	0.9182	0.0000	-4.2649	0.0000		
	0.8523	0.0000	-7.9880	0.0000		
	0.7609	0.0000	-13.6649	0.0000		
	0.6232	0.0000	-23.6425	0.0000		

Table D.3 Eigenvalues for Flight Condition 3

	Z-Domain		S-Domain		Freq.	Damping
	Real	Imag	Real	Imag	Rad/sec	
Open Loop Longitudinal			-0.0058	0.1429	0.1430	0.0406
			-0.0058	-0.1429	(phugoid)	
			-2.5741	0.0000		
			-6.2554	0.0000		
OW Longitudinal	0.9990	0.0007	-0.0519	0.0341	0.0621	0.8353
	0.9990	-0.0007	-0.0519	-0.0341		
	0.9452	0.0000	-2.8202	0.0000		
	0.8640	0.0639	-7.1738	3.6915	8.0678	0.8892
	0.8640	-0.0639	-7.1738	-3.6915		
	0.7958	0.0000	-11.4177	0.0000		
CRW Longitudinal	0.9985	0.0008	-0.0763	0.0379	0.0852	0.8955
	0.9985	-0.0008	-0.0763	-0.0379		
	0.9431	0.0000	-2.9269	0.0000		
	0.8975	0.0582	-5.3012	3.2401	6.2129	0.8532
	0.8975	-0.0582	-5.3012	-3.2401		
	0.7943	0.0000	-11.5159	0.0000		
	0.7475	0.0000	-14.5488	0.0000		
	0.0464	0.0000	-153.529	0.0000		
Open Loop Lateral			0.0194	0.0000		
			-0.2329	2.0604	2.0735	0.1123
			-0.2329	-2.0604	(dutch roll)	
			-2.4850	0.0000		
OW Lateral	0.9743	0.0000	-1.3042	0.0000		
	0.9577	0.0000	-2.1630	0.0000		
	0.9712	0.0454	-1.4041	2.3379	2.7272	0.5149
	0.9712	-0.0454	-1.4041	-2.3379		
	0.8613	0.0000	-7.4646	0.0000		
	0.8372	0.0000	-8.8828	0.0000		
CRW Lateral	0.9738	0.0000	-1.3295	0.0000		
	0.9581	0.0000	-2.1408	0.0000		
	0.9730	0.0486	-1.3086	2.4949	2.8173	0.4645
	0.9730	-0.0486	-1.3086	-2.4949		
	0.9192	0.0000	-4.2126	0.0000		
	0.8539	0.0000	-7.8956	0.0000		
	0.7599	0.0000	-13.7306	0.0000		
	0.6219	0.0000	-23.7492	0.0000		

Table D.4 Eigenvalues for Flight Condition 4

	Z-Domain		S-Domain		Freq.	Damping
	Real	Imag	Real	Imag	Rad/sec	
Open Loop Longitudinal			-0.0086	0.1028	0.1032	0.0829
			-0.0086	-0.1028	(phugoid)	
			-4.2157	1.5299	4.4848	0.9400
			-4.2157	-1.5299	(short period)	
OW Longitudinal	0.9992	0.0006	-0.3768	0.0298	0.0480	0.7843
	0.9992	-0.0006	-0.3768	-0.0298		
	0.9375	0.0000	-3.2272	0.0000		
	0.8699	0.1045	-6.6108	5.9750	8.9108	0.7419
	0.8699	-0.1045	-6.6108	-5.9750		
	0.7931	0.0000	-11.5890	0.0000		
CRW Longitudinal	0.9992	0.0006	-0.3768	0.0298	0.0480	0.7843
	0.9992	-0.0006	-0.3768	-0.0298		
	0.9393	0.0000	-3.1313	0.0000		
	0.9063	0.0885	-4.6845	4.8659	6.7545	0.6936
	0.9063	-0.0885	-4.6845	-4.8695		
	0.7903	0.0000	-11.7670	0.0000		
	0.7210	0.0000	-16.3530	0.0000		
	-0.0864	0.0000	-122.441	0.0000		
Open Loop Lateral			0.0030	0.0000		
			-2.3855	0.0000		
			-0.2222	2.5990	2.6085	0.0852
			-0.2222	-2.5990	(dutch roll)	
OW Lateral	0.9604	0.0186	-2.0122	0.9676	2.2328	0.9012
	0.9604	-0.0186	-2.0122	-0.9676		
	0.9483	0.0596	-2.5566	3.1365	4.0465	0.6318
	0.9483	-0.0596	-2.5566	-3.1365		
	0.9047	0.0000	-5.0076	0.0000		
	0.8488	0.0000	-8.1958	0.0000		
CRW Lateral	0.9603	0.0197	-2.0161	1.0253	2.2618	0.8914
	0.9603	-0.0197	-2.0161	1.0253		
	0.9436	0.0000	-2.9033	0.0000		
	0.9606	0.0690	-1.8835	3.5844	4.0491	0.4652
	0.9606	-0.0690	-1.8835	-3.5844		
	0.8706	0.0000	-6.9270	0.0000		
	0.7266	0.0000	-15.6959	0.0000		
	0.6056	0.0000	-25.0768	0.0000		

Table D.5 Eigenvalues for Flight Condition 5

	Z-Domain		S-Domain		Freq.	Damping
	Real	Imag	Real	Imag		Rad/sec
Open Loop Longitudinal			-0.0180	0.1957	0.1965	0.0914
			-0.0180	-0.1957	(phugoid)	
			-2.4356	0.0000		
			-5.5084	0.0000		
OW Longitudinal	0.9987	0.0010	-0.0636	0.0493	0.0805	0.7905
	0.9987	-0.0010	-0.0636	-0.0493		
	0.9491	0.0000	-2.6125	0.0000		
	0.8695	0.0395	-6.9429	2.2703	7.3047	0.9505
	0.8695	-0.0395	-6.9429	-2.2703		
	0.7981	0.0000	-11.2771	0.0000		
CRW Longitudinal	0.9987	0.0010	-0.0636	0.0493	0.0804	0.7905
	0.9987	-0.0010	-0.0636	-0.0493		
	0.9486	0.0000	-2.6401	0.0000		
	0.8990	0.0462	-5.2550	2.5692	5.8494	0.8984
	0.8990	-0.0462	-5.2550	-2.5692		
	0.7941	0.0000	-11.5277	0.0000		
	0.7625	0.0000	-13.5602	0.0000		
	0.1508	0.0000	-94.5814	0.0000		
Open Loop Lateral			0.0101	0.0000		
			-0.2109	1.7572	1.7698	0.1191
			-0.2109	-1.7572	(dutch roll)	
			-2.2895	0.0000		
OW Lateral	0.9822	0.0000	-0.8997	0.0000		
	0.9581	0.0000	-2.1387	0.0000		
	0.9777	0.0397	-1.0842	2.0296	2.3010	0.4718
	0.9777	-0.0397	-1.0842	-2.0296		
	0.8505	0.0000	-8.0939	0.0000		
	0.8327	0.0000	-9.1571	0.0000		
CRW Lateral	0.9820	0.0000	-0.9067	0.0000		
	0.9582	0.0000	-2.1333	0.0000		
	0.9786	0.0412	-1.0387	2.1015	2.3442	0.4431
	0.9786	-0.0412	-1.0387	-2.1015		
	0.9084	0.0000	-4.8047	0.0000		
	0.8475	0.0000	-8.2746	0.0000		
	0.7726	0.0000	-12.8966	0.0000		
	0.6275	0.0000	-23.2970	0.0000		

NASA National Aeronautics and Space Administration

Report Documentation Page

1. Report No.	2. Government Accession No.	3. Recipient's Catalog No.
NASA CR-4230		

4. Title and Subtitle

Detailed Design of a Ride Quality Augmentation System for Commuter Aircraft

5. Report Date

May 1989

6. Performing Organization Code

7. Author(s)

Reiner Suikat, Kent E. Donaldson, and David R. Downing

8. Performing Organization Report No.

KU-FRL-6132-7

10. Work Unit No.

505-61-41-02

9. Performing Organization Name and Address

The University of Kansas Center for Research, Inc.
Flight Research Laboratory
Lawrence, KS 66045-2969

11. Contract or Grant No.

NAG1-345

13. Type of Report and Period Covered

Contractor Report

12. Sponsoring Agency Name and Address

National Aeronautics and Space Administration
Langley Research Center
Hampton, VA 23665-5225

14. Sponsoring Agency Code

15. Supplementary Notes

Langley Technical Monitor: Earl C. Hastings, Jr.
Final Report

16. Abstract This report documents the continued design of a Ride Quality Augmentation System (RQAS) for commuter aircraft. The RQAS is designed for a Cessna 402B airplane, an 8 passenger prop twin representative of this class of airplanes. The purpose of the RQAS is the reduction of vertical and lateral accelerations of the aircraft due to atmospheric turbulence by the application of active control. The current phase of the project includes the detailed design of the hardware, i.e., the airplane modifications, the Ride Quality Instrumentation System (RQIS), and the required computer software. The aircraft modifications, consisting of the dedicated control surfaces and the hydraulic actuation system, have been designed at Cessna Aircraft under subcontract to KU-FRL. The instrumentation system, which consists of the sensor package, the flight computer, a Data Acquisition System (DAS), and the pilot and test engineer control panels, was designed by NASA LaRC. The overall system design and the design of the software, both for flight control algorithms and ground system checkouts, were KU's responsibility. The system performance is predicted from linear simulation results and from power spectral densities of the airplane response to a Dryden gust. The results indicate that vertical acceleration (rms) reductions of 45% and lateral acceleration (rms) reductions of more than 50% are possible.

17. Key Words (Suggested by Author(s))

Automatic Flight Controls
Ride Quality Augmentation
Commuter Aircraft

18. Distribution Statement

Unclassified - Unlimited

Subject Category 08

19. Security Classif. (of this report)	20. Security Classif. (of this page)	21. No. of pages	22. Price
Unclassified	Unclassified	120	A06

For sale by the National Technical Information Service, Springfield, Virginia 22161-2171